Engineering Applications of Artificial Intelligence 90 (2020) 103541

Contents lists available at ScienceDirect

Engineering Applications of Artificial Intelligence

journal homepage: www.elsevier.com/locate/engappai

Tunicate Swarm Algorithm: A new bio-inspired based metaheuristic paradigm for global optimization ☆

Satnam Kaur [a], Lalit K. Awasthi [a], A.L. Sangal [a], Gaurav Dhiman [b,*]

[a] Department of Computer Science and Engineering, Dr. B. R. Ambedkar National Institute of Technology, Jalandhar 144011, Punjab, India
[b] Department of Computer Science, Government Bikram College of Commerce, Patiala 147001, Punjab, India

ARTICLE INFO

Keywords:
Metaheuristics
Constrained optimization
Unconstrained optimization
Engineering design problems
Swarm intelligence

ABSTRACT

This paper introduces a bio-inspired metaheuristic optimization algorithm named Tunicate Swarm Algorithm (TSA). The proposed algorithm imitates jet propulsion and swarm behaviors of tunicates during the navigation and foraging process. The performance of TSA is evaluated on seventy-four benchmark test problems employing sensitivity, convergence and scalability analysis along with ANOVA test. The efficacy of this algorithm is further compared with several well-regarded metaheuristic approaches based on the generated optimal solutions. In addition, we also executed the proposed algorithm on six constrained and one unconstrained engineering design problems to further verify its robustness. The simulation results demonstrate that TSA generates better optimal solutions in comparison to other competitive algorithms and is capable of solving real case studies having unknown search spaces.
Note that the source codes of the proposed TSA algorithm are available at http://dhimangaurav.com/

1. Introduction

To minimize or maximize a function in terms of decision variables, optimization approach plays a significant role. Many real-life problems have a large number of solution spaces, which consists of non-linear constraints. Such problems also have high computational cost along with non-convex and complicated in nature (Singh and Dhiman, 2018a; Dhiman and Kumar, 2018c; Singh and Dhiman, 2018b; Dhiman and Kaur, 2018; Singh et al., 2018b; Dhiman and Kumar, 2018a; Kaur et al., 2018; Singh et al., 2018a). Hence, for solving such problems in terms of large number of variables and constraints are very complicated tasks. Further, local optimum solutions as obtained from various classical approaches do not guarantee for the best solution. To resolve these issues, numerous metaheuristic optimization algorithms are proposed by the researchers (Dhiman et al., 2018; Dhiman and Kumar, 2019b; Dhiman and Kaur, 2019b; Dhiman and Kumar, 2019a; Dhiman et al., 2019; Dhiman, 2019c), which are found to be very efficient for solving very complex problems. However, researchers have given more emphasize in developing of metaheuristic algorithms that are computationally inexpensive, flexible, and simple by nature.

In literature, two broad categories of metaheuristics algorithms are discussed, as *single solution based algorithm (SSBA)* and *population based algorithm (PBA)* (Dhiman and Kumar, 2017). In SSBA, a solution is randomly generated and improved until the optimal solution is obtained; whereas in case of PBA, solutions are randomly evolved in a given search space and try to improve until the optimal solution is obtained. However, most of the SSBAs are unable to reach at the level of global optimum solution due the reason of generating random solution. On the other hand, PBAs are able to find the global optimum. Due to this reason, researchers have attracted towards the PBAs nowadays (Singh et al., 2019; Dhiman, 2019a,b; Dehghani et al., 2019; Chandrawat et al., 2017; Singh and Dhiman, 2017; Dhiman and Kaur, 2017; Verma et al., 2018; Kaur and Dhiman, 2019; Dhiman and Kaur, 2019a; Dhiman and Kumar, 2019c; Garg and Dhiman, 2020).

Further PBAs are categorized, based on the theory of evolutionary algorithms (EAs), as logical behavior of physics algorithms, swarm intelligence of particles, and biological behavior of bio-inspired algorithms. Various EAs are motivated by natural processes, which include reproduction, mutation, recombination, and selection. The survival fitness of candidate in a population (i.e., a set of solutions) is the main basis of all these EAs. Algorithms that are based on the law of physics include the various rules of physics, such as electromagnetic force, gravitational force, heating and cooling of materials, and force of inertia. Algorithms that are biologically inspired mostly mimics the intelligence of swarms. Such kind of intelligence can be adopted among colonies of flocks, ants, and so on. Swarm intelligence based algorithms are very popular among the researchers due to its ease

☆ No author associated with this paper has disclosed any potential or pertinent conflicts which may be perceived to have impending conflict with this work. For full disclosure statements refer to https://doi.org/10.1016/j.engappai.2020.103541.

* Corresponding author.
E-mail address: gdhiman0001@gmail.com (G. Dhiman).

https://doi.org/10.1016/j.engappai.2020.103541
Received 19 December 2018; Received in revised form 18 November 2019; Accepted 5 February 2020
Available online xxxx
0952-1976/© 2020 Elsevier Ltd. All rights reserved.

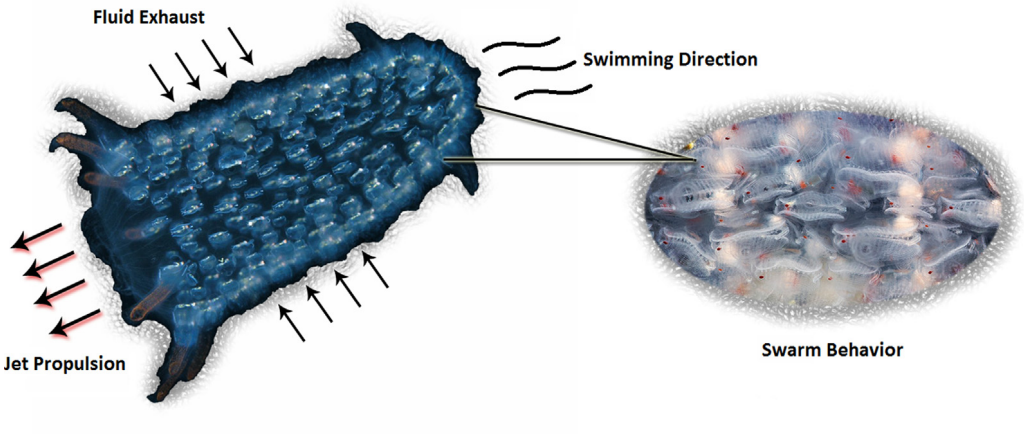

Fig. 1. Swarm behavior of tunicate in deep ocean.

of implementation. Its also requires very less number of parameters to be adjusted. Among this category of algorithms, Particle Swarm Optimization (PSO) (Kennedy and Eberhart, 1995) and Ant Colony Optimization (ACO) (Dorigo et al., 2006) are very well-known techniques for the global optimization problems. These kind of algorithms generally mimics the social behavior of fish schooling or bird flocking, where it is assumed that each particle moves around the search space and continuous update its current position *w.r.t.* the global position until satisfactory solution is found.

Optimization algorithms always requires to focus on *exploration* and *exploitation* of a search space (Alba and Dorronsoro, 2005) by maintaining good balancing between them. The exploration process in an algorithm investigates the various promising regions in a search space; whereas exploitation process searches the best solutions over the promising regions (Lozano and Garcia-Martinez, 2010). Hence, to achieve the optimal solutions or near to optimal solutions, these two processes are required to be tuned enough. Having availability of large number of such optimization algorithms, there is always a question raise for the requirement of development of more optimization algorithms. Its answer lies in *No Free Lunch (NFL)* theorem (Wolpert and Macready, 1997), which suggests that a specific optimization algorithm does not solve every problem, because every problem has its own complexity and nature. The *NFL* theorem inspires the researchers to design some new optimization algorithms, which can solve various domain of specific problems.

In this study, authors introduce a novel bio-inspired metaheuristic algorithm, named as Tunicate Swarm Algorithm (TSA), is proposed for optimizing non-linear constrained problems. It is inspired by the swarm behavior of tunicate to survive successfully in the depth of ocean. The main contributions of this work are as follows:

- A bio-inspired tunicate swarm algorithm (TSA) is proposed. The jet propulsion and swarm behaviors of tunicates are examined and mathematically modeled.
- The proposed TSA is implemented and tested on 74 benchmark test functions (i.e., classical, CEC-2015, and CEC-2017).
- The performance of the proposed TSA algorithm is compared with state-of-the-art metaheuristics.
- The efficiency of TSA algorithm is examined for solving the engineering design problems.

The rest of this paper is organized as follows: Section 2 presents the main inspiration and justification of the proposed algorithm. The proposed TSA algorithm is described in Section 3. The experimentation and simulations are presented in Section 4. Section 5 describes the applications of TSA on real-life engineering problems. Finally, the conclusion and future work is given in Section 6.

2. Inspiration

Tunicates are bright bio-luminescent, producing a pale blue–green light that can be seen more than many metres away. Tunicates are cylindrical-shaped which are open at one end and closed at the other (Berrill, 1950). Each tunicate is a few millimeters in size. There is a common gelatinous tunic in each tunicate which is helpful to join all of the individuals. However, each tunicate individually draws water from the surrounding sea and producing jet propulsion by its open end through atrial siphons. Tunicate is only animal to move around the ocean with such fluid jet like propulsion. This propulsion is powerful to migrate the tunicates vertically in ocean. Tunicates are often found at depth of 500–800 m and migrate upwards in the upper layer of surface water at night. The size of a tunicate varies from a few centimeter to more than 4 m (Davenport and Balazs, 1991). The most interesting fact of tunicate is their jet propulsion and swarm behaviors (see Fig. 1), which is the main motivation behind this paper.

2.1. Motivation

From past few decades, nature-inspired algorithms have gained significant attention from both industry as well as academia. Consequently, numerous algorithms have been provided by researchers after taking inspiration from the nature. In the catalogue of proposed nature-inspired approaches, a majority of algorithms are biology or bio-inspired as they are based on the notion of some characteristics of biological system. Among bio-inspired algorithms, a special class of algorithms have been developed by drawing inspiration from swarm intelligence. Population or Multiple-solution based swarm intelligence algorithms exhibit capability towards solving many real-world optimization problems due to their ability of thoroughly exploring the search space and returning the global optima. However, these approaches cannot solve all optimization problems as also stated by No Free Lunch theorem (Wolpert and Macready, 1997). This fact has motivated us to propose a new population based metaheuristic algorithm with the hope to solve several problems which are hard to solve with existing optimization techniques.

3. Tunicate swarm algorithm (TSA)

In this section, the inspiration and mathematical modeling of the proposed algorithm are described in detail.

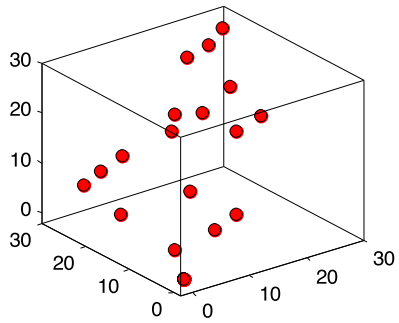

Fig. 2. Conflict avoidance between search agents.

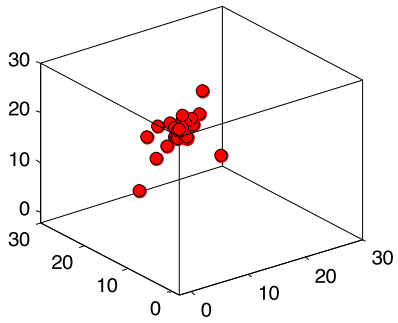

Fig. 3. Movement of search agents towards the best neighbor.

3.1. Mathematical model and optimization algorithm

Tunicate has an ability to find the location of food source in sea. However, there is no idea about the food source in the given search space. In this paper, two behaviors of tunicate are employed for finding the food source, i.e., optimum. These behaviors are jet propulsion and swarm intelligence.

To mathematically model the jet propulsion behavior, a tunicate should satisfied three conditions namely avoid the conflicts between search agents, movement towards the position of best search agent, and remains close to the best search agent. Whereas, the swarm behavior will update the positions of other search agents about the best optimal solution. The mathematical modeling of these behaviors is described in the preceding subsections.

3.1.1. Avoiding the conflicts among search agents

To avoid the conflicts between search agents (i.e., other tunicates), vector $\vec{A}$ is employed for the calculation of new search agent position as shown in Fig. 2.

$$\vec{A} = \frac{\vec{G}}{\vec{M}} \tag{1}$$

$$\vec{G} = c_2 + c_3 - \vec{F} \tag{2}$$

$$\vec{F} = 2 \cdot c_1 \tag{3}$$

However, $\vec{G}$ is the gravity force and $\vec{F}$ shows the water flow advection in deep ocean. The variables c_1, c_2, and c_3 are random numbers lie in the range of $[0, 1]$. $\vec{M}$ represents the social forces between search agents. The vector $\vec{M}$ is calculated as follows:

$$\vec{M} = \left| P_{min} + c_1 \cdot P_{max} - P_{min} \right| \tag{4}$$

where P_{min} and P_{max} represent the initial and subordinate speeds to make social interaction. In this work, the values of P_{min} and P_{max} are considered as 1 and 4, respectively. Note that the detailed sensitivity analysis of these parameters is discussed in Section 5.5.

3.1.2. Movement towards the direction of best neighbour

After avoiding the conflict between neighbors, the search agents are move towards the direction of best neighbour (see Fig. 3).

$$\vec{PD} = \left| \vec{FS} - r_{and} \cdot \vec{P_p}(x) \right| \tag{5}$$

where $\vec{PD}$ is the distance between the food source and search agent, i.e., tunicate, x indicates the current iteration, $\vec{FS}$ is the position of food source, i.e., optimum. Vector $\vec{P_p}(x)$ indicates the position of tunicate and r_{and} is a random number in range $[0, 1]$.

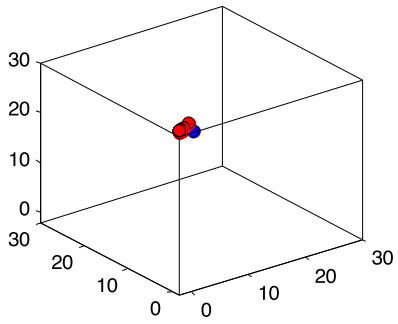

Fig. 4. Converge towards position of best search agent.

3.1.3. Converge towards the best search agent

The search agent can maintain its position towards the best search agent (i.e., food source) which is shown in Fig. 4.

$$\vec{P_p}(x) = \begin{cases} \vec{FS} + \vec{A} \cdot \vec{PD}, & \text{if } r_{and} \geq 0.5 \\ \vec{FS} - \vec{A} \cdot \vec{PD}, & \text{if } r_{and} < 0.5 \end{cases} \tag{6}$$

where $\vec{P_p}(x')$ is the updated position of tunicate with respect to the position of food source $\vec{FS}$.

3.1.4. Swarm behavior

In order to mathematically simulate the swarm behavior of tunicate, the first two optimal best solutions are saved and update the positions of other search agents according to the position of the best search agents. The following formula is proposed to define the swarm behavior of tunicate:

$$\vec{P_p}(x+1) = \frac{\vec{P_p}(x) + \vec{P_p}(x+1)}{2 + c_1} \tag{7}$$

Fig. 5 shows how search agents can updates their positions according to the position of $\vec{P}_p(x)$. The final position would be in a random place, within a cylindrical or cone-shaped, which is defined by the position of tunicate. The pseudo code of the proposed TSA algorithm is shown in Algorithm 1. There are some important points about the TSA algorithm which are described as:

- $\vec{A}$, $\vec{G}$, and $\vec{F}$ assist the solutions to behave randomly in a given search space and responsible to avoid the conflicts between different search agents.
- The possibility of better exploration and exploitation phases is done by the variations in vectors $\vec{A}$, $\vec{G}$, and $\vec{F}$.
- The jet propulsion and swarm behaviors of tunicate in a given search space defines the collective behavior of TSA algorithm (see Fig. 6).

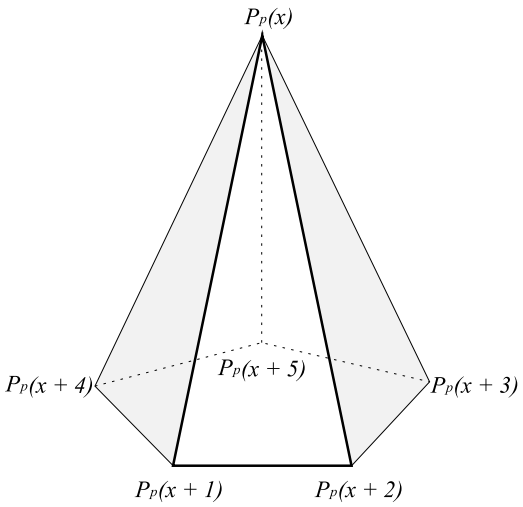

Fig. 5. 3D position vectors of tunicate.

3.2. Steps and flowchart of TSA

The steps and flowchart (see Fig. 7) of the proposed TSA are given below.

Step 1: Initialize the tunicate population $\vec{P}_p$.

Step 2: Choose the initial parameters and maximum number of iterations.

Step 3: Calculate the fitness value of each search agent.

Step 4: After computing the fitness value, the best search agent is explored in the given search space.

Step 5: Update the position of each search agent using Eq. (7).

Step 6: Adjust the updated search agent which goes beyond the boundary in a given search space.

Step 7: Compute the updated search agent fitness value. If there is a better solution than the previous optimal solution, then update P_p.

Step 8: If the stopping criterion is satisfied, then the algorithm stops. Otherwise, repeat the Steps 5–8.

Step 9: Return the best optimal solution which is obtained so far.

3.3. Computational complexity

In this subsection, the computational complexity of proposed TSA algorithm is discussed. Both the time and space complexities of the proposed algorithm are given below.

3.3.1. Time complexity

1. The initialization of population process needs $\mathcal{O}(n \times d)$ time, where n is the population size and d defines the dimension of a given test problem.
2. The agent fitness needs $\mathcal{O}(Max_{iterations} \times n \times d)$ time, where $Max_{iterations}$ is the maximum number of iterations.
3. TSA requires $\mathcal{O}(N)$ time, where N defines the jet propulsion and swarm behaviors of tunicate for better exploration and exploitation.

Hence, the total time complexity of TSA algorithm is $\mathcal{O}(Max_{iterations} \times n \times d \times N)$.

3.3.2. Space complexity

The space complexity of TSA algorithm is $\mathcal{O}(n \times d)$, which is considered as the maximum amount of space during its initialization process.

4. Experimental results and discussions

This section describes the simulation and experimentation of TSA on seventy-four standard benchmark test functions. The detailed description of these benchmark test functions are discussed below. Further, the results are analyzed and compared with well-known metaheuristics.

4.1. Description of benchmark test functions

The seventy-four benchmark test functions are applied on the proposed algorithm to demonstrate its applicability and efficiency. These functions are divided into six main categories: Unimodal

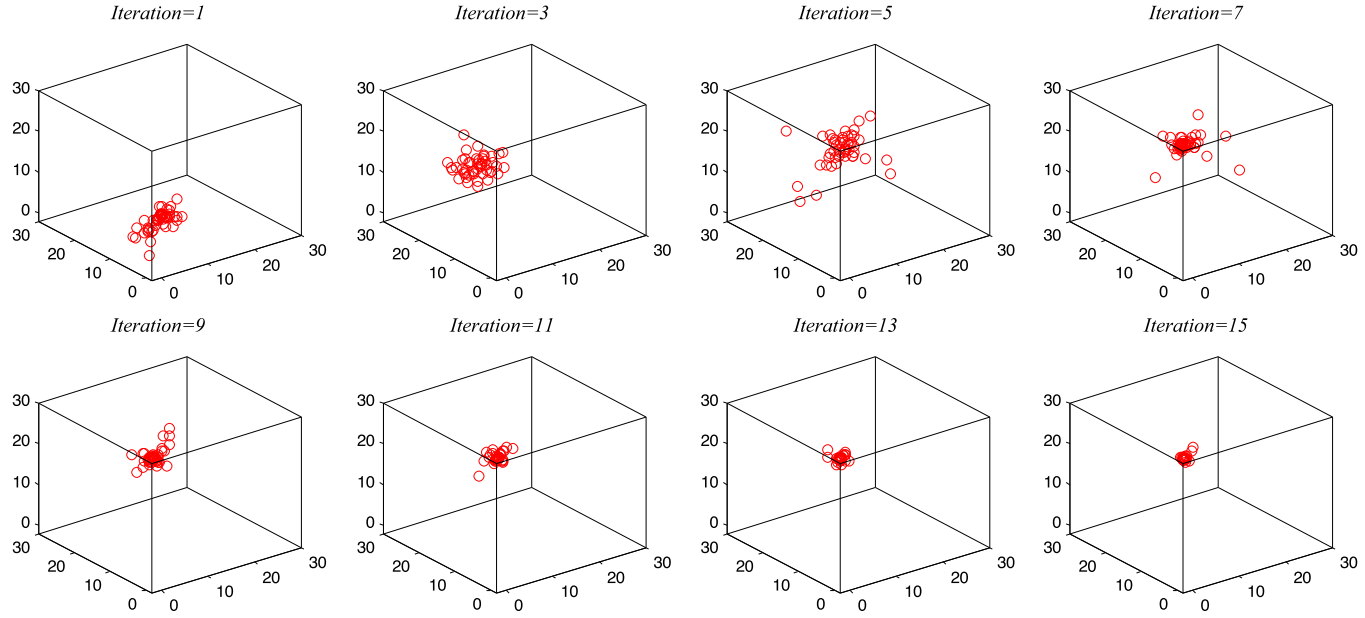

Fig. 6. Jet propulsion and swarm behaviors of tunicate in two-dimensional environment.

Algorithm 1 Tunicate Swarm Algorithm

Input: Tunicate population $\vec{P}_p$
Output: Optimal fitness value $\vec{FS}$
procedure TSA
Initialize the parameters $\vec{A}, \vec{G}, \vec{F}, \vec{M}$, and $Max_{iterations}$
  Set $P_{min} \leftarrow 1$
  Set $P_{max} \leftarrow 4$
  Set $Swarm \leftarrow 0$
  while $(x < Max_{iterations})$ **do**
    for i $\leftarrow$ 1 to 2 **do** /* Looping for compute swarm behavior */
      $\vec{FS} \leftarrow$**ComputeFitness(**$\vec{P}_p$**)** /* Calculate the fitness values of each search agent using **ComputeFitness** function*/
  /* Jet propulsion behavior */
      $c_1, c_2, c_3, r_{and} \leftarrow Rand()$ /* Rand() is a function to generate the random number in range [0, 1] */
      $\vec{M} \leftarrow \left| P_{min} + c_1 \times P_{max} - P_{min} \right|$
      $\vec{F} \leftarrow 2 \times c_1$
      $\vec{G} \leftarrow c_2 + c_3 - \vec{F}$
      $\vec{A} \leftarrow \vec{G} / \vec{M}$
      $\vec{PD} \leftarrow \text{ABS}(\vec{FS} - r_{and} \times \vec{P_p}(x))$
  /* Swarm behavior */
      if$(r_{and} \leq 0.5)$ **then**
        $Swarm \leftarrow Swarm + \vec{FS} + \vec{A} \times \vec{PD}$
      else
        $Swarm \leftarrow Swarm + \vec{FS} - \vec{A} \times \vec{PD}$
      end if
    end for
    $\vec{P_p}(x) \leftarrow Swarm/(2 + c_1)$
    $Swarm \leftarrow 0$
    Update the parameters $\vec{A}, \vec{G}, \vec{F}$, and $\vec{M}$
    $x \leftarrow x + 1$
  end while
return $\vec{FS}$
end procedure

procedure ComputeFitness($\vec{P}_p$)
  for i $\leftarrow$ 1 to n **do** /* Here, n represents the dimension of a given problem */
    $FIT_p[i] \leftarrow FitnessFunction(P_p(\vec{i}, :))$ /* Calculate the fitness of each individual */
  end for
  $FIT_{P_{best}} \leftarrow$ **BEST**$(FIT_p[])$ /* Calculate the best fitness value using **BEST** function */
return $FIT_{P_{best}}$
end procedure

procedure BEST(FIT_p)
  $Best \leftarrow FIT_p[0]$
  for i $\leftarrow$ 1 to n **do**
    if$(FIT_p[i] < Best)$ **then**
      $Best \leftarrow FIT_p[i]$
    end if
  end for
return $Best$ /* Return the best fitness value */
end procedure

(Digalakis and Margaritis, 2001), Multimodal (Yang, 2010), Fixed-dimension Multimodal (Digalakis and Margaritis, 2001; Yang, 2010), Composite (Liang et al., 2005), CEC-2015 (Chen et al., 2014), and CEC-2017 (Awad et al., 2016) test functions. The description of these test functions is given in Appendix.

4.2. Experimental setup

The proposed TSA is compared with well-known metaheuristic algorithms namely Spotted Hyena Optimizer (SHO) (Dhiman and Kumar, 2017), Grey Wolf Optimizer (GWO) (Mirjalili et al., 2014), Particle Swarm Optimization (PSO) (Kennedy and Eberhart, 1995), Multi-verse Optimizer (MVO) (Mirjalili et al., 2016), Sine Cosine Algorithm (SCA) (Mirjalili, 2016), Gravitational Search Algorithm (GSA) (Rashedi et al., 2009), Genetic Algorithm (GA) (Holland, 1992), Emperor Penguin Optimizer (EPO) (Dhiman and Kumar, 2018b), and jSO (Brest et al., 2017). Table 1 shows the parameter settings of all algorithms. The experimentation has been done on Matlab R2017b version using 64 bit Core i5 processor with 3.20 GHz and 16 GB main memory.

4.3. Performance comparison

The performance of proposed TSA algorithm is compared with state-of-the-art optimization algorithms on unimodal, multimodal, fixed-dimension multimodal, composite, CEC-2015, and CEC-2017 benchmark test functions. The average and standard deviation is considered

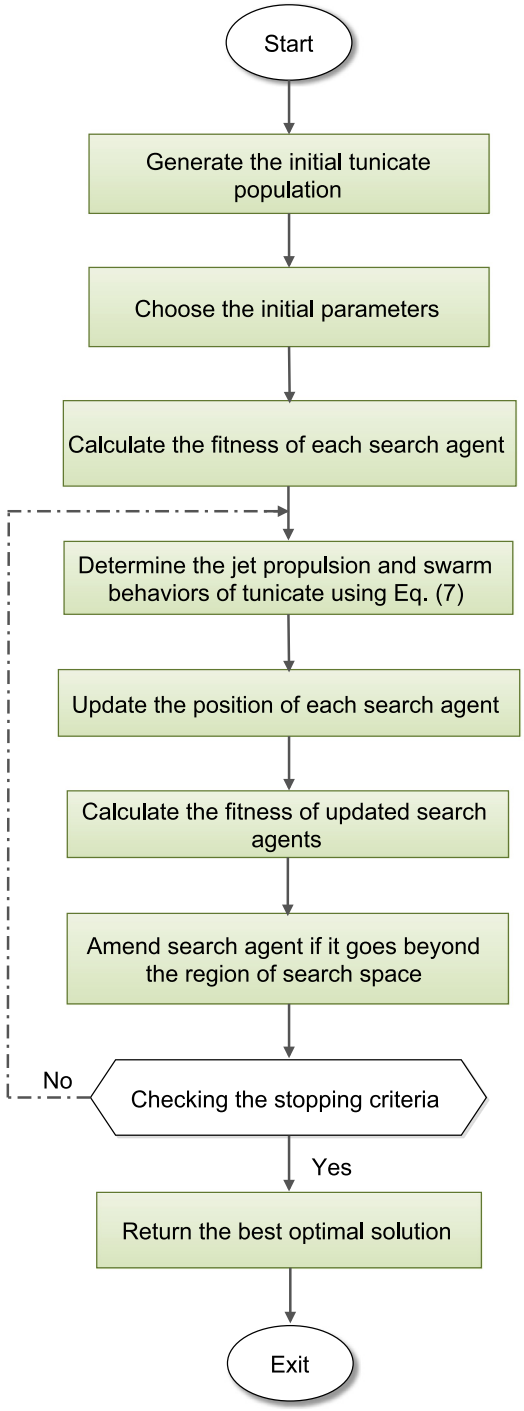

Fig. 7. Flowchart of the proposed TSA algorithm.

as the best optimal solution on benchmark functions. For benchmark test functions, the proposed algorithm simulates 30 independent runs in which each run employs 1000 number of iterations.

4.3.1. Evaluation of test functions $F_1 - F_7$

Table 2 shows the mean and standard deviation of best obtained optimal solution on unimodal benchmark test functions. For F_1, F_2, and F_3 benchmark test functions, SHO is the best optimizer whereas TSA is the second best optimizer in terms of average and standard deviation. TSA obtains better competitor results on F_4, F_5, F_6, and F_7 benchmark test functions. It is seen from results that TSA is very effective and competitive as compared with other metaheuristic algorithms.

Table 1
Parameters settings.

#	Algorithms	Parameters	Values
1.	Tunicate Swarm Algorithm (TSA)	Search agents	80
		Parameter P_{min}	1
		Parameter P_{max}	4
		Number of generations	1000
2.	Spotted Hyena Optimizer (SHO)	Search agents	80
		Control parameter ($\vec{h}$)	[5, 0]
		$\vec{M}$ constant	[0.5, 1]
		Number of generations	1000
3.	Grey Wolf Optimizer (GWO)	Search agents	80
		Control parameter ($\vec{a}$)	[2, 0]
		Number of generations	1000
4.	Particle Swarm Optimization (PSO)	Number of particles	80
		Inertia coefficient	0.75
		Cognitive and social coeff	1.8, 2
		Number of generations	1000
5.	Multi-Verse Optimizer (MVO)	Search agents	80
		Wormhole existence Prob.	[0.2, 1]
		Traveling distance rate	[0.6, 1]
		Number of generations	1000
6.	Sine Cosine Algorithm (SCA)	Search agents	80
		Number of elites	2
		Number of generations	1000
7.	Gravitational Search Algorithm (GSA)	Search agents	80
		Gravitational constant	100
		Alpha coefficient	20
		Number of generations	1000
8.	Genetic Algorithm (GA)	Population size	80
		Crossover	0.9
		Mutation	0.05
		Number of generations	1000
9.	Emperor Penguin Optimizer (EPO)	Search agents	80
		Temperature profile (T')	[1, 1000]
		$\vec{A}$ constant	[−1.5, 1.5]
		Function $S()$	[0, 1.5]
		Parameter M	2
		Parameter f	[2, 3]
		Parameter l	[1.5, 2]
		Number of generations	1000

4.3.2. Evaluation of test functions $F_8 - F_{23}$

Tables 3 and 4 show the computational performance of above-mentioned algorithms on multimodal benchmark test functions ($F_8 - F_{13}$) and fixed-dimension multimodal benchmark test functions ($F_{14} - F_{23}$), respectively. These tables show that TSA is able to find near optimal solution on nine benchmark test problems (i.e., $F_8, F_{10}, F_{13}, F_{14}, F_{15}, F_{17}, F_{18}, F_{19}$, and F_{22}). For F_9, F_{11}, and F_{16} benchmark test functions, SHO provides near optimal results than TSA algorithm. TSA is the second best optimizer on these benchmark test functions. PSO generates best optimal solution for F_{12} and F_{20} benchmark test functions. For F_{21} benchmark test function, GWO and TSA are the first and second best metaheuristic optimization algorithms, respectively. The results show that TSA obtains very competitive results in majority of the benchmark test problems.

4.3.3. Evaluation of test functions $F_{24} - F_{29}$

Table 5 shows the experimental results on composite benchmark test functions. The results show that over 3 out of 6 benchmark functions, TSA obtains better than the other approaches. GSA obtains best optimal solution for F_{24} benchmark test function. For F_{28} and F_{29} benchmark test functions, SHO provides better optimal results than TSA algorithm. However, TSA is the third best optimization algorithm for F_{24}, F_{28}, and F_{29} benchmark test functions.

Table 2
Mean and standard deviation of best optimal solution for 30 independent runs on unimodal benchmark test functions.

F	TSA		SHO		GWO		PSO		MVO		SCA		GSA		GA		EPO	
	Ave	*Std*	*Ave*	*Std*	*Ave*	*Std*	*Ave*	*Std*	*Ave*	*Std*	*Ave*	*Std*	*Ave*	*Std*	*Ave*	*Std*	*Ave*	*Std*
F_1	7.71E−38	7.00E−21	**0.00E+00**	**0.00E+00**	4.61E−23	7.37E−23	4.98E−09	1.40E−08	2.81E−01	1.11E−01	3.55E−02	1.06E−01	1.16E−16	6.10E−17	1.95E−12	2.01E−11	5.71E−28	8.31E−29
F_2	8.48E−39	5.92E−41	**0.00E+00**	**0.00E+00**	1.20E−34	1.30E−34	7.29E−04	1.84E−03	3.96E−01	1.41E−01	3.23E−05	8.57E−05	1.70E−01	9.29E−01	6.53E−18	5.10E−17	6.20E−40	3.32E−40
F_3	1.15E−21	6.70E−21	**0.00E+00**	**0.00E+00**	1.00E−14	4.10E−14	1.40E+01	7.13E+00	4.31E+01	8.97E+00	4.91E+03	3.89E+03	4.16E+02	1.56E+02	7.70E−10	7.36E−09	2.05E−19	9.17E−20
F_4	**1.33E−23**	**1.15E−22**	7.78E−12	8.96E−12	2.02E−14	2.43E−14	6.00E−01	1.72E−01	8.80E−01	2.50E−01	1.87E+01	8.21E+00	1.12E+00	9.89E−01	9.17E+01	5.67E+01	4.32E−18	3.98E−19
F_5	**5.13E+00**	**4.76E−03**	8.59E+00	5.53E−01	2.79E+01	1.84E+00	4.93E+01	3.89E+01	1.18E+02	1.43E+02	7.37E+02	1.98E+03	3.85E+01	3.47E+01	5.57E+02	4.16E+01	5.07E+00	4.90E−01
F_6	**7.10E−21**	**1.12E−25**	2.46E−01	1.78E−01	6.58E−01	3.38E−01	9.23E−09	1.78E−08	3.15E−01	9.98E−02	4.88E+00	9.75E−01	1.08E−16	4.00E−17	3.15E−01	9.98E−02	7.01E−19	4.39E−20
F_7	**3.72E−07**	**5.09E−07**	3.29E−05	2.43E−05	7.80E−04	3.85E−04	6.92E−02	2.87E−02	2.02E−02	7.43E−03	3.88E−02	5.79E−02	7.68E−01	2.77E+00	6.79E−04	3.29E−03	2.71E−05	9.26E−06

Table 3
Mean and standard deviation of best optimal solution for 30 independent runs on multimodal benchmark test functions.

F	TSA		SHO		GWO		PSO		MVO		SCA		GSA		GA		EPO	
	Ave	*Std*	*Ave*	*Std*	*Ave*	*Std*	*Ave*	*Std*	*Ave*	*Std*	*Ave*	*Std*	*Ave*	*Std*	*Ave*	*Std*	*Ave*	*Std*
F_8	**−8.93E+02**	4.15E+01	−1.16E+02	**2.72E+01**	−6.14E+02	9.32E+01	−6.01E+02	1.30E+02	−6.92E+02	9.19E+01	−3.81E+02	2.83E+01	−2.75E+02	5.72E+01	−5.11E+02	4.37E+01	−8.76E+02	5.92E+01
F_9	5.70E−03	1.46E−03	**0.00E+00**	**0.00E+00**	4.34E−01	1.66E+00	4.72E+01	1.03E+01	1.01E+02	1.89E+01	2.23E+01	3.25E+01	3.35E+01	1.19E+01	1.23E−01	4.11E+01	6.90E−01	4.81E−01
F_{10}	**9.80E−19**	4.51E−12	2.48E+00	1.41E+00	1.63E−14	**3.14E−15**	3.86E−02	2.11E−01	1.15E+00	7.87E−01	1.55E+01	8.11E+00	8.25E−09	1.90E−09	5.31E−11	1.11E−10	8.03E−16	2.74E−14
F_{11}	1.00E−07	7.46E−07	**0.00E+00**	**0.00E+00**	2.29E−03	5.24E−03	5.50E−03	7.39E−03	5.74E−01	1.12E−01	3.01E−01	2.89E−01	8.19E+00	3.70E+00	3.31E−06	4.23E−05	4.20E−05	4.73E−04
F_{12}	6.07E−06	2.72E−05	3.68E−02	1.15E−02	3.93E−02	2.42E−02	**1.05E−10**	**2.06E−10**	1.27E+00	1.02E+00	5.21E+01	2.47E+02	2.65E−01	3.14E−01	9.16E−08	4.88E−07	5.09E−03	3.75E−03
F_{13}	**0.00E+00**	**0.00E+00**	9.29E−01	9.52E−02	4.75E−01	2.38E−01	4.03E−03	5.39E−03	6.60E−02	4.33E−02	2.81E+02	8.63E+02	5.73E−32	8.95E−32	6.39E−02	4.49E−02	0.00E+00	0.00E+00

Table 4
Mean and standard deviation of best optimal solution for 30 independent runs on fixed-dimension multimodal benchmark test functions.

F	TSA		SHO		GWO		PSO		MVO		SCA		GSA		GA		EPO	
	Ave	*Std*	*Ave*	*Std*	*Ave*	*Std*	*Ave*	*Std*	*Ave*	*Std*	*Ave*	*Std*	*Ave*	*Std*	*Ave*	*Std*	*Ave*	*Std*
F_{14}	**1.03E+00**	2.11E−04	9.68E+00	3.29E+00	3.71E+00	3.86E+00	2.77E+00	2.32E+00	9.98E+01	**9.14E−12**	1.26E+00	6.86E−01	3.61E+00	2.96E+00	4.39E+00	4.41E−02	1.08E+00	4.11E−02
F_{15}	**8.10E−05**	**4.06E−05**	9.01E−03	1.06E−03	3.66E−02	7.60E−02	9.09E−03	2.38E−03	7.15E−02	1.26E−01	1.01E−02	3.75E−03	6.84E−02	7.37E−02	7.36E−02	2.39E−03	8.21E−03	4.09E−03
F_{16}	−1.02E+00	1.99E−09	**−1.03E+00**	**2.86E−11**	−1.02E+00	7.02E−09	−1.02E+00	0.00E+00	−1.02E+00	4.74E−08	−1.02E+00	3.23E−05	−1.02E+00	0.00E+00	−1.02E+00	4.19E−07	−1.02E+00	9.80E−07
F_{17}	**3.96E−01**	3.71E−09	3.97E−01	2.46E−01	3.98E−01	7.00E−07	3.97E−01	9.03E−16	3.98E−01	1.15E−07	3.98E−01	7.61E−04	3.98E−01	1.13E−16	3.98E−01	**3.71E−17**	3.98E−01	5.39E−05
F_{18}	**3.00E+00**	**3.56E−09**	3.00E+00	9.05E+00	3.00E+00	7.16E−06	3.00E+00	6.59E−05	3.00E+00	1.48E+01	3.00E+00	2.25E−05	3.00E+00	3.24E−02	3.00E+00	6.33E−07	3.00E+00	1.15E−08
F_{19}	**−3.89E+00**	3.01E−09	−3.71E+00	4.39E−01	−3.84E+00	1.57E−03	−3.80E+00	**3.37E−15**	−3.77E+00	3.53E−07	−3.75E+00	2.55E−03	−3.86E+00	4.15E−01	−3.81E+00	4.37E−10	−3.86E+00	6.50E−07
F_{20}	−2.97E+00	2.10E−01	−1.44E+00	5.47E−01	−3.27E+00	7.27E−02	**−3.32E+00**	2.66E−01	−3.23E+00	**5.37E−02**	−2.84E+00	3.71E−01	−1.47E+00	5.32E−01	−2.39E+00	4.37E−01	−2.81E+00	7.11E−01
F_{21}	−7.01E+00	1.23E+00	−2.08E+00	**3.80E−01**	**−9.65E+00**	1.54E+00	−7.54E+00	2.77E+00	−7.38E+00	2.91E+00	−2.28E+00	1.80E+00	−4.57E+00	1.30E+00	−5.19E+00	2.34E+00	−8.07E+00	2.29E+00
F_{22}	**−13.07E+00**	3.15E−03	−1.61E+00	**2.04E−04**	−1.04E+00	2.73E−04	−8.55E+00	3.08E+00	−8.50E+00	3.02E+00	−3.99E+00	1.99E+00	−6.58E+00	2.64E+00	−2.97E+00	1.37E−02	−10.01E+00	3.97E−02
F_{23}	−3.51E+00	3.10E−03	−1.68E+00	2.64E−01	**−1.05E+01**	**1.81E−04**	−9.19E+00	2.52E+00	−8.41E+00	3.13E+00	−4.49E+00	1.96E+00	−9.37E+00	2.75E+00	−3.10E+00	2.37E+00	−3.41E+00	1.11E−02

Table 5
Mean and standard deviation of best optimal solution for 30 independent runs on composite benchmark test functions.

F	TSA		SHO		GWO		PSO		MVO		SCA		GSA		GA		EPO	
	Ave	*Std*	*Ave*	*Std*	*Ave*	*Std*	*Ave*	*Std*	*Ave*	*Std*	*Ave*	*Std*	*Ave*	*Std*	*Ave*	*Std*	*Ave*	*Std*
F_{24}	1.33E+02	4.10E+01	2.30E+02	1.37E+02	8.39E+01	8.42E+01	6.00E+01	8.94E+01	1.40E+02	1.52E+02	1.20E+02	3.11E+01	**4.49E−17**	**2.56E−17**	5.97E+02	1.34E+02	2.33E+02	9.22E+01
F_{25}	**3.00E+01**	2.02E+01	4.08E+02	9.36E+01	1.48E+02	3.78E+01	2.44E+02	1.73E+02	2.50E+02	1.44E+02	1.14E+02	**1.84E+00**	2.03E+02	4.47E+02	4.09E+02	2.10E+01	4.10E+01	3.09E+01
F_{26}	**3.34E+02**	4.36E+01	3.39E+02	**3.14E+01**	3.53E+02	5.88E+01	3.39E+02	8.36E+01	4.05E+02	1.67E+02	3.89E+02	5.41E+01	3.67E+02	8.38E+01	9.30E+02	8.31E+01	3.39E+02	5.03E+01
F_{27}	**2.40E+02**	**1.13E+01**	7.26E+02	1.21E+02	4.23E+02	1.14E+02	4.49E+02	1.42E+02	3.77E+02	1.28E+02	4.31E+02	2.94E+01	5.32E+02	1.01E+02	4.97E+02	3.24E+01	3.44E+02	2.17E+01
F_{28}	1.20E+02	4.00E+01	**1.06E+02**	**1.38E+01**	1.36E+02	2.13E+02	2.40E+02	4.25E+02	2.45E+02	9.96E+01	1.56E+02	8.30E+01	1.44E+02	1.31E+02	1.90E+02	5.03E+01	1.46E+02	7.06E+01
F_{29}	6.41E+02	6.00E+02	**5.97E+02**	**4.98E+00**	8.26E+02	1.74E+02	8.22E+02	1.80E+02	8.33E+02	1.68E+02	6.06E+02	1.66E+02	8.13E+02	1.13E+02	6.65E+02	3.37E+02	7.43E+02	9.09E+02

Table 6
Mean and standard deviation of best optimal solution for 30 independent runs on CEC-2015 benchmark test functions.

F	TSA		SHO		GWO		PSO		MVO		SCA		GSA		GA		EPO	
	Ave	*Std*	*Ave*	*Std*	*Ave*	*Std*	*Ave*	*Std*	*Ave*	*Std*	*Ave*	*Std*	*Ave*	*Std*	*Ave*	*Std*	*Ave*	*Std*
$CEC-1$	**1.24E+05**	1.13E+06	2.28E+06	2.18E+06	2.02E+06	2.08E+06	4.37E+05	**4.73E+05**	1.47E+06	2.63E+06	6.06E+05	5.02E+05	7.65E+06	3.07E+06	3.20E+07	8.37E+06	1.50E+05	1.21E+06
$CEC-2$	5.55E+05	1.00E+06	3.13E+05	4.19E+05	5.65E+06	6.03E+06	9.41E+03	1.08E+04	1.97E+04	1.46E+04	1.43E+04	1.03E+04	7.33E+08	2.33E+08	**4.58E+03**	**1.09E+03**	6.70E+06	1.34E+08
$CEC-3$	**3.20E+02**	2.36E−03	3.20E+02	3.76E−02	3.20E+02	7.08E−02	3.20E+02	8.61E−02	3.20E+02	9.14E−02	3.20E+02	3.19E−02	3.20E+02	7.53E−02	3.20E+02	**1.11E−05**	3.20E+02	1.16E−03
$CEC-4$	5.70E+02	3.30E+01	4.11E+02	1.71E+01	4.16E+02	1.03E+01	**4.09E+02**	**3.96E+00**	4.26E+02	1.17E+01	4.18E+02	1.03E+01	4.42E+02	7.72E+00	4.39E+02	7.25E+00	4.10E+02	5.61E+01
$CEC-5$	8.75E+02	3.18E+02	9.13E+02	1.85E+02	9.20E+02	**1.78E+02**	**8.65E+02**	2.16E+02	1.33E+03	3.45E+02	1.09E+03	2.81E+02	1.76E+03	2.30E+02	1.75E+03	2.79E+02	9.81E+02	2.06E+02
$CEC-6$	2.10E+03	1.28E+04	1.29E+04	1.15E+04	2.26E+04	2.45E+04	**1.86E+03**	**1.93E+03**	7.35E+03	3.82E+03	3.82E+03	2.44E+03	2.30E+04	2.41E+04	3.91E+06	2.70E+06	2.05E+03	1.05E+04
$CEC-7$	**7.02E+02**	**3.17E−02**	7.02E+02	6.76E−01	7.02E+02	7.07E−01	7.02E+02	7.75E−01	7.02E+02	1.10E+00	7.02E+02	9.40E−01	7.06E+02	9.07E−01	7.08E+02	1.32E+00	7.02E+02	5.50E−01
$CEC-8$	**1.41E+03**	1.01E+03	1.86E+03	1.98E+03	3.49E+03	2.04E+03	3.43E+03	2.77E+03	9.93E+03	8.74E+03	2.58E+03	**1.61E+03**	6.73E+03	3.36E+03	6.07E+05	4.81E+05	1.47E+03	2.34E+03
$CEC-9$	**1.00E+03**	1.65E+01	1.00E+03	1.43E−01	1.00E+03	1.28E−01	1.00E+03	7.23E−02	1.00E+03	2.20E−01	1.00E+03	**5.29E−02**	1.00E+03	9.79E−01	1.00E+03	5.33E+00	1.00E+03	1.51E+01
$CEC-10$	**1.19E+03**	4.42E+04	2.00E+03	2.73E+03	4.00E+03	2.82E+03	3.27E+03	1.84E+03	8.39E+03	1.12E+04	2.62E+03	**1.78E+03**	9.91E+03	8.83E+03	3.42E+05	1.74E+05	1.23E+03	2.51E+04
$CEC-11$	**1.34E+03**	**1.21E+01**	1.38E+03	2.42E+01	1.40E+03	5.81E+01	1.35E+03	1.12E+02	1.37E+03	8.97E+01	1.39E+03	5.42E+01	1.35E+03	1.11E+02	1.41E+03	7.73E+01	1.35E+03	1.41E+01
$CEC-12$	**1.30E+03**	5.35E+00	1.30E+03	7.89E−01	1.30E+03	**6.69E−01**	1.30E+03	6.94E−01	1.30E+03	9.14E−01	1.30E+03	8.07E−01	1.31E+03	1.54E+00	1.31E+03	2.05E+00	1.30E+03	7.50E+00
$CEC-13$	**1.30E+03**	**4.40E−07**	1.30E+03	2.76E−04	1.30E+03	1.92E−04	1.30E+03	5.44E−03	1.30E+03	1.04E−03	1.30E+03	2.43E−04	1.30E+03	3.78E−03	1.35E+03	4.70E+01	1.30E+03	6.43E−05
$CEC-14$	**3.16E+03**	1.76E+03	4.25E+03	1.73E+03	7.29E+03	2.45E+03	7.10E+03	3.12E+03	7.60E+03	1.29E+03	7.34E+03	2.47E+03	7.51E+03	1.52E+03	9.30E+03	**4.04E+02**	3.22E+03	2.12E+03
$CEC-15$	**1.60E+03**	3.45E+01	1.60E+03	3.76E+00	1.61E+03	4.94E+00	1.60E+03	**2.66E−07**	1.61E+03	1.13E+01	1.60E+03	1.80E−02	1.62E+03	3.64E+00	1.64E+03	1.12E+01	1.60E+03	5.69E+01

Table 7
Mean and standard deviation of best optimal solution for 30 independent runs on CEC-2017 benchmark test functions.

F	TSA		SHO		GWO		PSO		MVO		SCA		GSA		GA		jSO	
	Ave	*Std*	*Ave*	*Std*	*Ave*	*Std*	*Ave*	*Std*	*Ave*	*Std*	*Ave*	*Std*	*Ave*	*Std*	*Ave*	*Std*	*Ave*	*Std*
$C-1$	2.70E+04	1.21E+07	2.38E+05	2.28E+07	2.12E+05	2.18E+07	4.47E+04	4.83E+06	1.57E+05	2.73E+07	6.16E+04	5.12E+06	7.75E+05	3.17E+07	3.30E+06	8.47E+07	**0.00E+00**	**0.00E+00**
$C-2$	5.82E+05	3.41E+09	3.23E+04	4.29E+06	5.75E+05	6.13E+07	9.51E+03	1.18E+05	1.07E+03	1.56E+05	1.53E+04	1.13E+05	7.43E+07	2.43E+09	4.68E+03	1.19E+04	**0.00E+00**	**0.00E+00**
$C-3$	3.30E+02	2.38E−05	3.30E+02	3.86E−03	3.30E+02	7.18E−03	3.30E+02	8.71E−03	3.30E+02	9.24E−03	3.30E+02	3.29E−03	3.30E+02	7.63E−03	3.30E+02	1.21E−06	**0.00E+00**	**0.00E+00**
$C-4$	**3.40E+01**	4.62E+02	4.21E+02	1.81E+02	4.26E+02	1.13E+02	4.19E+02	3.06E+01	4.36E+02	1.27E+02	4.28E+02	1.13E+02	4.52E+02	7.82E+02	4.49E+02	7.35E+02	5.62E+01	**4.88E+01**
$C-5$	**1.40E+01**	2.19E+03	9.23E+02	1.95E+03	9.30E+02	1.88E+03	8.75E+02	2.26E+03	1.43E+04	3.55E+04	1.19E+04	2.91E+03	1.86E+03	2.40E+03	1.85E+03	2.89E+03	1.64E+01	**3.46E+00**
$C-6$	2.17E+04	2.13E+05	1.39E+04	1.25E+05	2.36E+03	2.55E+05	1.96E+03	1.03E+04	7.45E+03	3.92E+04	3.92E+04	2.54E+04	2.40E+04	2.51E+05	3.01E+05	2.80E+07	**1.09E−06**	**2.62E−06**
$C-7$	7.12E+02	**4.49E−02**	7.12E+02	6.86E−02	7.12E+02	7.17E−02	7.12E+03	7.85E−02	7.12E+02	1.20E+01	7.12E+03	9.50E−02	7.16E+02	9.17E−02	7.18E+02	1.42E+01	**6.65E+01**	3.47E+00
$C-8$	**1.56E+01**	3.00E+04	1.96E+03	1.08E+04	3.59E+04	2.14E+04	3.53E+03	2.87E+04	9.03E+03	8.84E+05	2.68E+04	1.71E+04	6.83E+03	3.46E+04	6.17E+04	4.91E+08	1.70E+01	**3.14E+00**
$C-9$	1.10E+03	1.50E+02	1.10E+04	1.53E−02	1.10E+04	1.38E−02	1.10E+03	7.33E−02	1.10E+04	2.30E−01	1.10E+03	5.39E−03	1.10E+03	9.89E−02	1.10E+04	5.43E+01	**0.00E+00**	**0.00E+00**
$C-10$	**1.32E+03**	1.50E+04	2.10E+03	2.83E+04	4.10E+04	2.92E+04	3.37E+03	1.94E+04	8.49E+04	1.22E+05	2.72E+03	1.88E+04	9.01E+04	8.93E+04	3.52E+04	1.84E+06	3.14E+03	**3.67E+02**
$C-11$	**1.45E+01**	2.76E+01	1.48E+03	2.52E+02	1.50E+04	5.91E+02	1.45E+03	1.22E+03	1.47E+04	8.07E+02	1.49E+04	5.52E+02	1.45E+04	1.21E+03	1.51E+03	7.83E+02	2.79E+01	**3.33E+00**
$C-12$	**1.40E+03**	6.79E+00	1.40E+04	7.99E−02	1.40E+03	**6.79E−02**	1.40E+04	6.04E−02	1.40E+03	9.24E−02	1.40E+05	8.17E−02	1.41E+03	1.64E+01	1.41E+06	2.15E+01	1.68E+03	5.23E+02
$C-13$	**1.40E+01**	**5.49E−06**	1.40E+02	2.86E−05	1.40E+06	1.02E−05	1.40E+03	5.54E−04	1.40E+04	1.14E−04	1.40E+03	2.53E−05	1.40E+04	3.88E−04	1.45E+02	4.80E+02	3.06E+01	2.12E+01
$C-14$	3.33E+03	2.00E+03	4.35E+04	1.83E+04	7.39E+03	2.55E+04	7.20E+03	3.22E+04	7.70E+04	1.39E+04	7.44E+04	2.57E+04	7.61E+03	1.62E+04	9.40E+03	4.14E+03	**2.50E+01**	**1.87E+00**
$C-15$	1.70E+03	9.86E+01	1.70E+03	3.86E+01	1.71E+04	4.04E+01	1.70E+03	**2.76E−05**	1.71E+06	1.23E+02	1.70E+03	1.90E−03	1.72E+06	3.74E+01	1.74E+06	1.22E+01	**2.39E+01**	2.49E+00
$C-16$	2.46E+04	3.20E+08	3.28E+05	3.18E+09	3.02E+06	3.08E+09	5.37E+05	5.73E+08	2.47E+05	3.63E+09	7.06E+05	6.02E+09	8.65E+05	4.07E+09	4.20E+06	9.37E+09	**4.51E+02**	**1.38E+02**
$C-17$	8.48E+05	7.03E+06	4.13E+04	5.19E+04	6.65E+06	7.03E+05	8.41E+04	2.08E+04	2.97E+04	2.46E+04	2.43E+05	2.03E+03	8.33E+06	3.33E+07	5.58E+03	2.09E+03	**2.83E+02**	**8.61E+01**
$C-18$	4.20E+02	7.47E−05	4.20E+02	4.76E−04	4.20E+02	8.08E−04	4.20E+02	9.61E−04	4.20E+02	8.14E−04	4.20E+03	4.19E−04	4.20E+02	8.53E−04	4.20E+03	**2.11E−07**	**2.43E+01**	2.02E+00
$C-19$	4.05E+02	5.60E+02	5.11E+03	2.71E+02	5.16E+02	2.03E+02	**1.09E+01**	**4.90E−01**	5.26E+02	2.17E+02	5.18E+03	2.03E+02	5.42E+02	8.72E+02	5.39E+03	8.25E+02	1.41E+01	2.26E+00
$C-20$	**1.11E+02**	4.07E+01	8.13E+03	2.85E+01	8.20E+02	**2.78E+00**	7.65E+02	3.16E+01	2.33E+03	4.45E+02	2.09E+03	3.81E+01	2.76E+04	3.30E+02	2.75E+03	3.79E+01	1.40E+02	7.74E+01
$C-21$	3.02E+03	2.16E+04	2.29E+03	2.15E+04	3.26E+04	3.45E+05	2.86E+03	2.93E+03	8.35E+04	4.82E+03	4.82E+04	3.44E+04	3.30E+04	3.41E+04	4.91E+06	3.70E+07	**2.19E+02**	**3.77E+00**
$C-22$	**8.02E+02**	**5.47E−02**	8.02E+02	7.76E−01	8.02E+03	8.07E−01	8.02E+02	8.75E−01	8.02E+02	2.10E+01	8.02E+03	8.40E−01	8.06E+03	8.07E−02	8.08E+02	2.32E+00	1.49E+03	1.75E+03
$C-23$	3.35E+03	1.31E+03	2.86E+03	2.98E+04	4.49E+04	3.04E+04	4.43E+04	3.77E+04	8.93E+04	9.74E+04	3.58E+03	2.61E+04	7.73E+03	4.36E+04	7.07E+04	5.81E+06	**4.30E+02**	**6.24E+00**
$C-24$	2.00E+04	6.76E+01	2.00E+04	2.43E−02	2.00E+04	2.28E−02	2.00E+04	7.23E−03	2.00E+04	3.20E−02	2.00E+04	**6.29E−03**	2.00E+04	8.79E−02	2.00E+04	6.33E+01	**5.07E+02**	4.13E+00
$C-25$	**2.22E+02**	6.46E+05	3.00E+04	3.73E+04	5.00E+04	3.82E+04	4.27E+04	2.84E+04	9.39E+04	2.12E+05	3.62E+04	2.78E+04	8.91E+04	6.83E+04	4.42E+06	2.74E+06	4.81E+02	**2.80E+00**
$C-26$	**1.00E+03**	**2.26E+01**	2.38E+04	3.42E+02	2.40E+04	6.81E+02	2.35E+05	2.12E+03	2.37E+04	9.97E+02	2.39E+04	6.42E+02	2.35E+04	2.11E+03	2.41E+04	8.73E+02	1.13E+03	5.62E+01
$C-27$	2.30E+04	1.40E+00	2.30E+04	8.89E−02	2.30E+04	**7.69E−02**	2.30E+04	7.94E−02	2.30E+04	8.14E−02	2.30E+04	9.07E−02	2.31E+04	3.54E+01	2.31E+04	3.05E+00	**5.11E+02**	1.11E+01
$C-28$	5.30E+04	**6.11E−06**	5.30E+04	3.76E−05	5.30E+04	3.92E−05	5.30E+04	6.44E−04	5.30E+04	2.04E−04	5.30E+04	3.43E−05	5.30E+04	4.78E−04	5.35E+04	4.70E+02	**4.60E+02**	6.84E+00
$C-29$	**3.20E+02**	4.66E+03	5.25E+04	2.73E+04	8.29E+03	3.45E+04	8.10E+04	4.12E+04	8.60E+03	2.29E+05	8.34E+04	3.47E+05	8.51E+03	2.52E+04	8.30E+04	5.04E+03	3.63E+02	**1.32E+01**
$C-30$	**2.60E+04**	5.55E+01	2.60E+04	4.76E+01	2.61E+04	5.94E+01	2.60E+04	**3.66E−04**	2.61E+04	2.13E+02	2.60E+04	2.80E−03	2.62E+04	4.64E+01	2.64E+04	2.12E+02	6.01E+05	2.99E+04

4.3.4. Evaluation of IEEE CEC-2015 test functions (CEC1 – CEC15)

Table 6 reveals the performance of TSA and other optimization algorithms on IEEE CEC-2015 benchmark test functions. It is seen from Table 6 that TSA generates better results for $CEC-1, CEC-3, CEC-7, CEC-8, CEC-9, CEC-10, CEC-11, CEC-12, CEC-13, CEC-14$, and $CEC-15$ benchmark test functions. For $CEC-4, CEC-5$, and $CEC-6$ benchmark test functions, PSO performance is better than other algorithms in terms of fitness value. TSA is the second best optimizer on these test functions.

4.3.5. Evaluation of IEEE CEC-2017 test functions (C1–C30)

Table 7 reveals the performance of proposed TSA algorithm and other competitive algorithms on IEEE CEC-2017 benchmark test functions. The results show that TSA generates best optimal solution for $C-4, C-5, C-8, C-10, C-11, C-12, C-13, C-20, C-22, C-25, C-26, C-29, C-30$ benchmark test functions.

4.4. Convergence analysis

The convergence curves of proposed TSA algorithm is shown in Fig. 8. It is analyzed that TSA is very competitive over benchmark functions. TSA algorithm has three different behaviors of convergence. In the starting stage of iteration process, the convergence efficiency of TSA algorithm is more quickly in a given search space. In second stage of iteration, TSA converges with the direction of optimum when final iteration reaches. The last iteration process shows the express convergence behavior from the initial stage of iterations. The results show that TSA algorithm maintains a balance between exploration and exploitation. The search history is another metric to determine how TSA explores and exploits in a given search space. The search history of TSA is depicted in Fig. 8. It is observed from Fig. 8 that TSA explore most promising area in the given search space for benchmark test functions. For unimodal test functions, the sample points are sparsely distributed in the non-promising area. Whereas, the most of sample points are distributed around the promising area for multimodal and fixed-dimension multimodal test functions. This is due to the difficulty level of these test functions. TSA does not stuck in local optima and explores the entire search space. The distribution of sample points is around the true optimal solution, which ensures its exploitation capability. Therefore, TSA has both exploration and exploitation capability.

4.5. Sensitivity analysis

The proposed TSA algorithm employs four parameters, i.e., maximum number of iterations, number of search agents, parameter P_{min}, and parameter P_{max}.

1. Maximum number of iterations: TSA algorithm was simulate for different number of iteration processes. The values of $Max_{iteration}$ used in this work are 100, 500, 800, and 1000. Table 8 and Fig. 9(a) show the variations of iterations on various benchmark test functions. The results show that TSA converges towards the optimal solution when the number of iterations is increased.
2. Number of search agents: TSA algorithm was simulate for different values of search agent (i.e., 30, 50, 80, 100). Table 9 and Fig. 9(b) show the variations of different number of search agents on benchmark test functions. It is analyzed from Fig. 9(b) that the value of fitness function decreases when number of search agents increases.
3. Variation in parameter P_{min}: To investigate the effect of parameter P_{min}, TSA algorithm was run for different values of P_{min} keeping other parameters fixed. The values of P_{min} used in experimentation are 1, 2, 3, and 4. Table 10 and Fig. 9(c) show the variation of P_{min} on different benchmark test functions. The results show that TSA generates better optimal results when the value of P_{min} is set to 1.
4. Variation in parameter P_{max}: To investigate the effect of parameter P_{max}, TSA was simulate for 1, 2, 3, and 4 by keeping other parameters fixed. Table 11 and Fig. 9(d) show the effect of P_{max} on various benchmark test functions. It is seen that TSA generates better optimal results when the value of P_{max} is fixed to 4.

4.6. Scalability study

This subsection describes the effect of scalability on various test functions by using proposed TSA. The dimensionality of the test functions is made to vary as 30, 50, 80, and 100. Fig. 10 shows the performance of TSA algorithm on scalable benchmark test functions. It is observed that the performance of TSA is not too much degraded when the dimensionality of search space is increased. The results reveal that the performance of TSA is least affected with the increase in dimensionality of search space. This is due to better capability of the proposed TSA for balancing between exploration and exploitation.

4.7. Statistical testing

Apart from standard statistical analysis such as mean and standard deviation, Analysis of Variance (ANOVA) test has been conducted. ANOVA test is used to determine whether the results obtained from proposed algorithm are different from other competitor algorithms in a statistically significant way. The sample size for ANOVA test is 30 with 95% confidence of interval. A $p-$ value determine whether the given algorithm is statistically significant or not. If $p-$ value of the given algorithm is less than 0.05, then the corresponding algorithm is statistically significant. Table 12 shows the analysis of ANOVA test on the benchmark test functions. It is observed from Table 12 that the $p-$ value obtained from TSA is much smaller than 0.05 for all the benchmark test functions. Therefore, the proposed TSA is statistical different from the other competitor algorithms.

5. TSA for engineering design problems

TSA algorithm is tested on six constrained and one unconstrained engineering design problems. These problems are pressure vessel, speed reducer, welded beam, tension/compression spring, 25-bar truss, rolling element bearing, and displacement of loaded structure.

5.1. Constrained engineering design problems

This subsection describes six constrained engineering design problems to validate the performance of proposed algorithm.

5.1.1. Pressure vessel design problem

This problem was first proposed by Kannan and Kramer (1994) to minimize the total cost of material, forming, and welding of a cylindrical vessel. The schematic view of pressure vessel design problem is shown in Fig. 11. There are four design variables:

- T_s (z_1, thickness of the shell).
- T_h (z_2, thickness of the head).
- R (z_3, inner radius).
- L (z_4, length of the cylindrical section without considering the head).

Apart from these, R and L are continuous variables whereas T_s and T_h are integer values which are multiples of 0.0625 in. The mathematical

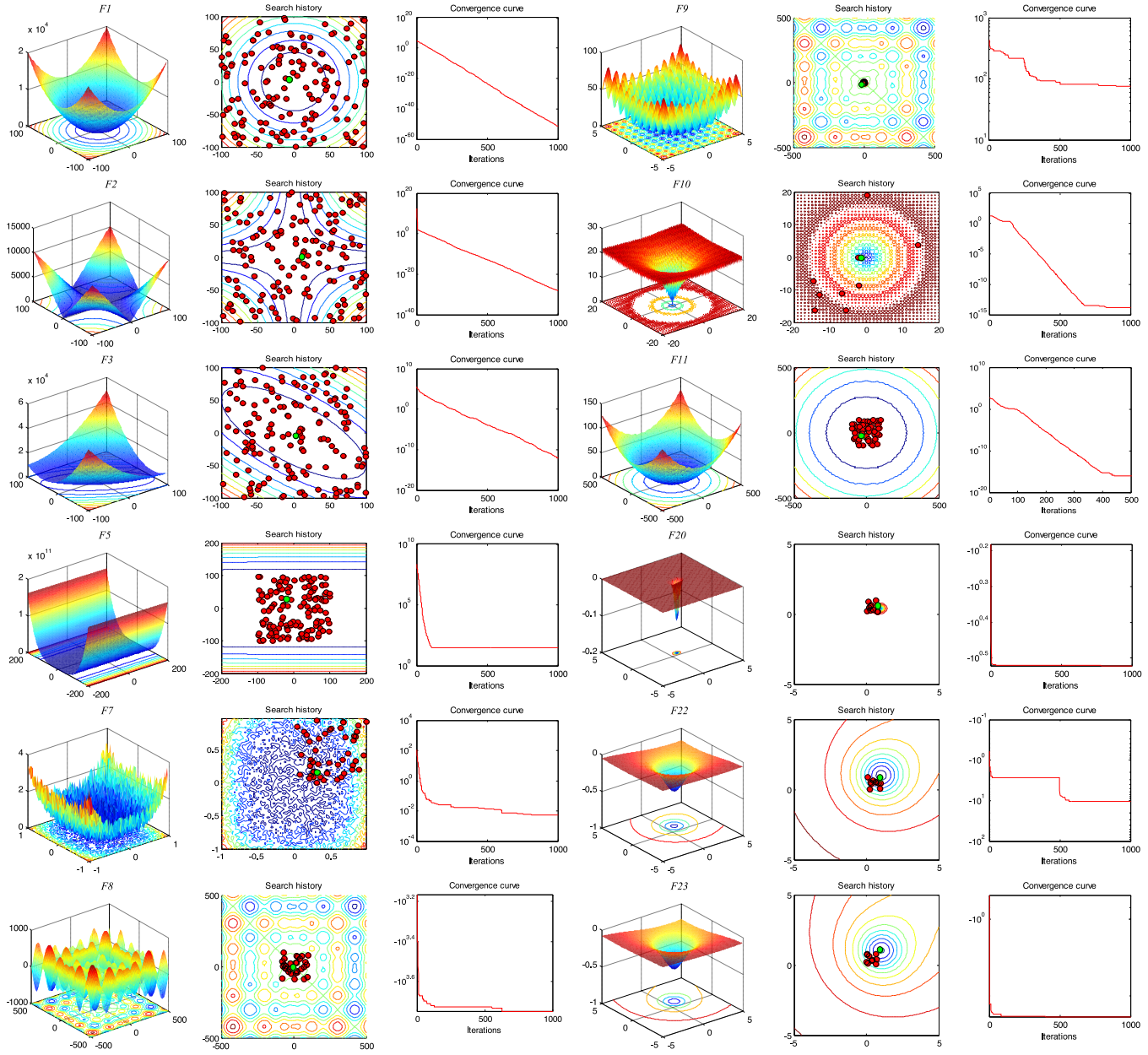

Fig. 8. Convergence analysis of the proposed TSA and search history on benchmark test problems.

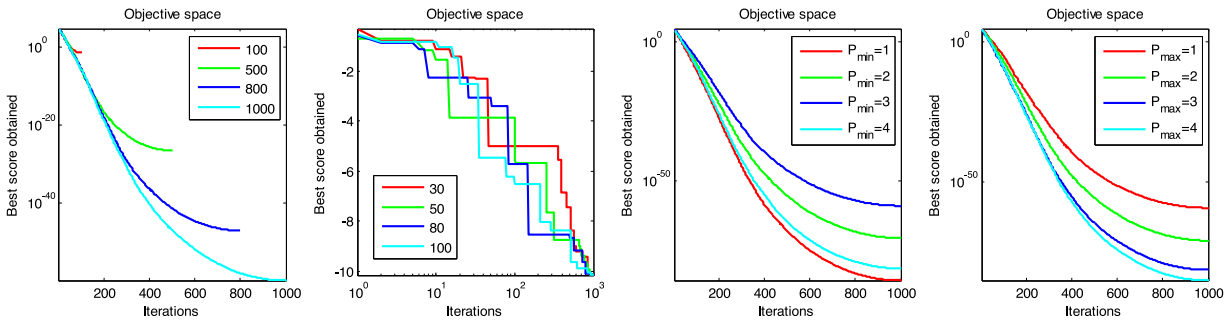

Fig. 9. Sensitivity analysis of the proposed TSA algorithm for, (a) Number of iterations; (b) Number of search agents; (c) Control parameter P_{min}; (d) Control parameter P_{max}.

Table 8
The obtained optimal values on unimodal, multimodal, fixed-dimension multimodal, composite, and CEC-2015 benchmark test functions using different simulation runs (i.e., 100, 500, 800, and 1000).

Iterations	Functions						
	F_1	F_5	F_{11}	F_{17}	F_{23}	F_{24}	$CEC-1$
100	8.19E−12	5.01E+02	7.29E−05	5.21E−03	−2.42E+01	4.48E+04	1.29E+08
500	4.41E−19	5.07E+02	4.22E−07	8.90E−03	−2.91E+02	4.16E+04	5.51E+07
800	3.07E−23	5.26E+02	5.11E−04	7.77E−08	−3.10E+02	3.91E+04	4.00E+05
1000	**5.10E−31**	**4.00E+00**	**2.19E−17**	**7.08E−12**	**−3.42E+00**	**9.75E+01**	**4.40E+02**

Table 9
The obtained optimal values on unimodal, multimodal, fixed-dimension multimodal, composite, and CEC-2015 benchmark test functions where number of iterations is fixed as 1000. The number of search agents are varied from 30 to 100.

Search agents	Functions						
	F_1	F_5	F_{11}	F_{17}	F_{23}	F_{24}	$CEC-1$
30	5.51E−10	5.11E+00	5.11E−02	5.26E−02	−2.51E+00	1.30E+02	2.66E+06
50	5.42E−15	5.11E+02	3.11E−02	9.10E−01	−2.81E+00	4.20E+02	1.20E+05
80	**7.27E−30**	**4.00E+00**	**3.20E−09**	**5.15E−04**	**−4.49E+00**	**4.12E+01**	**1.57E+03**
100	5.91E−13	5.40E+00	8.10E−01	6.00E−02	−3.12E+00	2.86E+03	2.75E+06

Table 10
The obtained optimal values on unimodal, multimodal, fixed-dimension multimodal, composite, and CEC-2015 benchmark test functions where number of iterations and search agents are fixed as 1000 and 80, respectively. The parameter P_{min} is varied from [1, 2, 3, 4].

P_{min}	Functions						
	F_1	F_5	F_{11}	F_{17}	F_{23}	F_{24}	$CEC-1$
1	**1.10E−31**	**5.00E+00**	**4.45E−07**	**5.01E−03**	**−3.50E+00**	**1.01E+01**	**8.24E+03**
2	9.93E−19	9.09E+01	8.88E−02	1.70E−00	−2.11E+00	5.00E+03	9.59E+07
3	2.11E−12	5.60E+01	2.00E−01	8.01E−01	−2.88E+00	4.45E+03	3.48E+07
4	1.52E−20	3.48E+01	8.17E−02	4.00E−01	−3.16E+00	7.97E+03	4.17E+06

Table 11
The obtained optimal values on unimodal, multimodal, fixed-dimension multimodal, composite, and CEC-2015 benchmark test functions where number of iterations and search agents are fixed as 1000 and 80, respectively. The parameter f is fixed as 1. The parameter P_{max} is varied from [1, 2, 3, 4].

P_{max}	Functions						
	F_1	F_5	F_{11}	F_{17}	F_{23}	F_{24}	$CEC-1$
1	5.46E−19	7.18E+01	4.41E−02	9.90E−00	−2.22E+00	1.70E+03	2.40E+05
2	1.71E−20	2.36E+00	1.21E−03	7.56E−01	−2.93E+00	3.17E+03	2.61E+04
3	8.15E−23	5.05E+00	7.90E−03	5.00E−01	−3.07E+00	3.81E+03	1.00E+06
4	**1.17E−28**	**1.00E+00**	**2.00E−09**	**2.47E−02**	**−3.51E+00**	**1.99E+01**	**4.05E+02**

formulation of this problem is described below:

Consider $\vec{z} = [z_1\ z_2\ z_3\ z_4] = [T_s\ T_h\ R\ L]$,

Minimize $f(\vec{z}) = 0.6224 z_1 z_3 z_4 + 1.7781 z_2 z_3^2 + 3.1661 z_1^2 z_4 + 19.84 z_1^2 z_3$,

Subject to:

$$g_1(\vec{z}) = -z_1 + 0.0193 z_3 \le 0,$$

$$g_2(\vec{z}) = -z_3 + 0.00954 z_3 \le 0,$$

$$g_3(\vec{z}) = -\pi z_3^2 z_4 - \frac{4}{3}\pi z_3^3 + 1{,}296{,}000 \le 0,$$

$$g_4(\vec{z}) = z_4 - 240 \le 0,$$

where,

$$1 \times 0.0625 \le z_1,\ z_2 \le 99 \times 0.0625,\ 10.0 \le z_3,\ z_4 \le 200.0. \tag{8}$$

Table 13 shows the comparison between TSA and other competitor algorithms such as EPO, SHO, GWO, PSO, MVO, SCA, GSA, and GA. TSA obtains optimal solution at point $z_{1-4} = (0.778090, 0.383230, 40.315050, 200.00000)$ and its fitness value is $f(z_{1-4}) = 5870.9550$. It can be clear from table that TSA algorithm is capable to find an optimal design with low cost.

The obtained statistical results of this problem are given in Table 14. It can be analyzed from table that TSA achieves optimal values in terms of best, mean, and median as compared to other algorithms. The convergence analysis of TSA on this problem for best optimal design is shown in Fig. 12.

5.1.2. Speed reducer design problem

The speed reducer design problem is an engineering design problem. It has seven design variables (Gandomi and Yang, 2011) as shown in Fig. 13. The main objective of this design problem is to minimize the weight of speed reducer with subject to the following constraints (Mezura-Montes and Coello, 2005):

- Bending stress of the gear teeth.
- Surface stress.
- Transverse deflections of the shafts.
- Stresses in the shafts.

There are seven design variables ($z_1 - z_7$) such as face width (b), module of teeth (m), number of teeth in the pinion (p), length of the first shaft between bearings (l_1), length of the second shaft between bearings (l_2), diameter of first (d_1) shafts, and diameter of second shafts (d_2). The

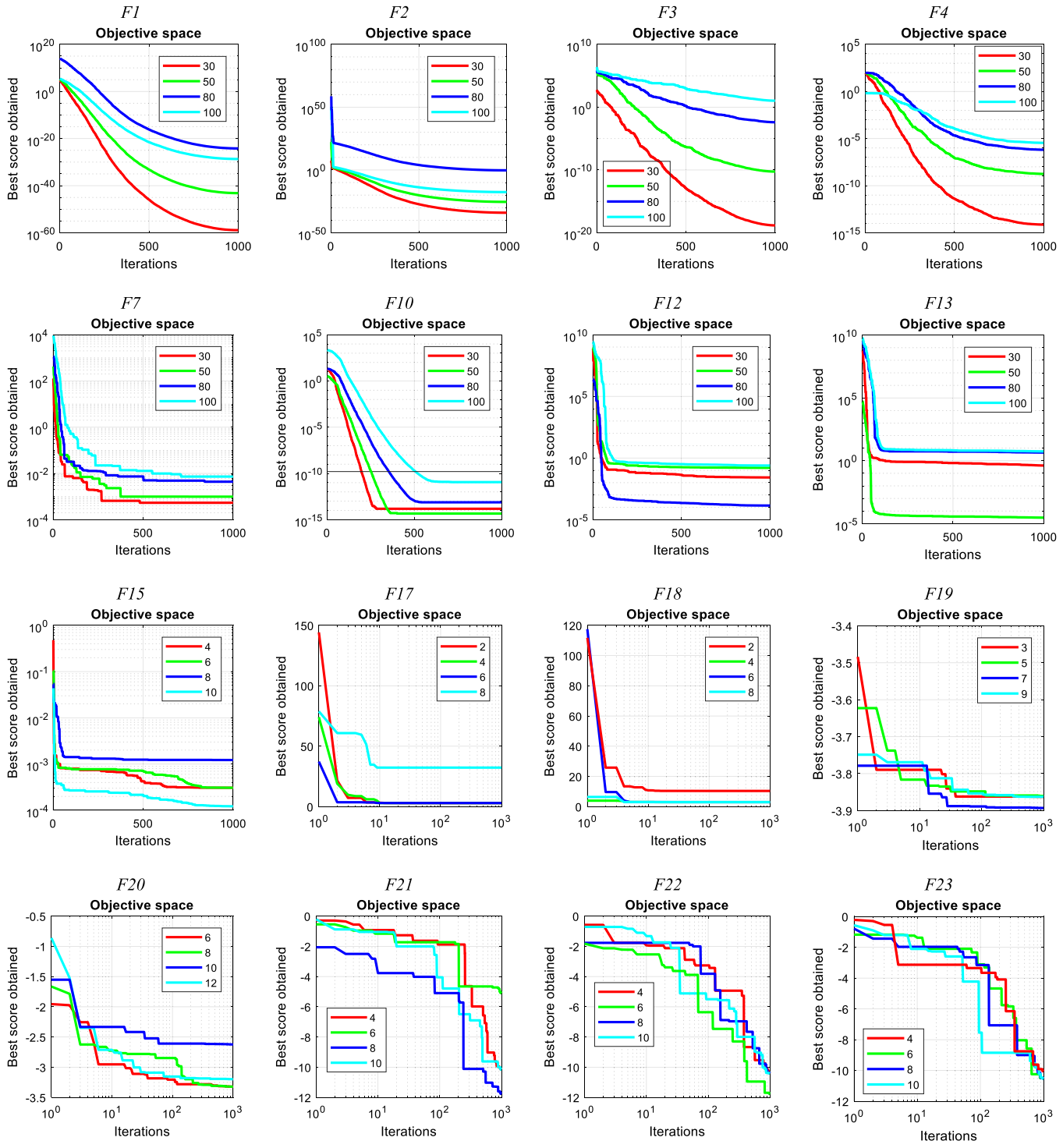

Fig. 10. Effect of scalability on the performance of TSA algorithm.

mathematical formulation of this problem is described as follows:

$$
\begin{aligned}
&\text{Consider } \vec{z} = [z_1\ z_2\ z_3\ z_4\ z_5\ z_6\ z_7] = [b\ m\ p\ l_1\ l_2\ d_1\ d_2],\\
&\text{Minimize } f(\vec{z}) = 0.7854 z_1 z_2^2 (3.3333 z_3^2 + 14.9334 z_3 - 43.0934)\\
&- 1.508 z_1 (z_6^2 + z_7^2) + 7.4777 (z_6^3 + z_7^3) + 0.7854 (z_4 z_6^2 + z_5 z_7^2),\\
&\text{Subject to:}\\
&g_1(\vec{z}) = \frac{27}{z_1 z_2^2 z_3} - 1 \le 0,\\
&g_2(\vec{z}) = \frac{397.5}{z_1 z_2^2 z_3^2} - 1 \le 0,
\end{aligned}
\tag{9}
$$

$$
\begin{aligned}
&g_3(\vec{z}) = \frac{1.93 z_4^3}{z_2 z_6^4 z_3} - 1 \le 0,\\
&g_4(\vec{z}) = \frac{1.93 z_5^3}{z_2 z_7^4 z_3} - 1 \le 0,\\
&g_5(\vec{z}) = \frac{[(745(z_4/z_2 z_3))^2 + 16.9 \times 10^6]^{1/2}}{110 z_6^3} - 1 \le 0,\\
&g_6(\vec{z}) = \frac{[(745(z_5/z_2 z_3))^2 + 157.5 \times 10^6]^{1/2}}{85 z_7^3} - 1 \le 0,
\end{aligned}
$$

Table 12
Analysis of Variance (ANOVA) test results.

F	$p-$ value	TSA	SHO	GWO	PSO	MVO	SCA	GSA	GA	EPO
F_1	4.70E−11	SHO, GWO, PSO, SCA, GSA, GA, EPO	TSA, GWO, PSO, MVO, SCA, GSA, GA, EPO	TSA, SHO, PSO, SCA, GSA, GA, EPO	TSA, SHO, GWO, MVO, SCA, GSA, GA, EPO	TSA, SHO, PSO, SCA, GA, EPO	TSA, SHO, GWO, GSA, GA, EPO	TSA, SHO, GWO, PSO, MVO, SCA, GA, EPO	TSA, SHO, GWO, MVO, SCA, GSA, EPO	TSA, SHO, GWO, MVO, SCA, GSA, GA
F_2	6.66E−20	SHO, GWO, PSO, MVO, SCA, GA, EPO	TSA, GWO, PSO, MVO, SCA, GSA, GA, EPO	TSA, SHO, PSO, SCA, GSA, GA, EPO	TSA, GWO, MVO, SCA, GSA, GA, EPO	TSA, GWO, PSO, SCA, GSA, GA	TSA, SHO, PSO, GSA, GA, EPO	TSA, SHO, GWO, PSO, MVO, SCA, GA, EPO	TSA, SHO, GWO, PSO, SCA, EPO	TSA, SHO, GWO, PSO, MVO, SCA, GSA
F_3	1.50E−46	SHO, GWO, PSO, SCA, GSA, GA, EPO	TSA, GWO, PSO, SCA, GSA, GA	TSA, SHO, MVO, SCA, GSA, GA, EPO	TSA, SHO, GWO, MVO, SCA, GSA, GA, EPO	TSA, GWO, PSO, SCA, GSA, GA, EPO	TSA, SHO, MVO, GA, EPO	TSA, SHO, GWO, PSO, MVO, SCA, EPO	TSA, SHO, GWO, PSO, MVO, SCA, GSA, EPO	TSA, SHO, PSO, MVO, SCA, GA
F_4	8.82E−80	SHO, GWO, PSO, MVO, SCA, GSA, GA, EPO	TSA, GWO, PSO, MVO, SCA, GSA, GA, EPO	TSA, SHO, PSO, MVO, SCA, GSA, GA, EPO	TSA, SHO, GWO, SCA, GSA, GA, EPO	TSA, SHO, GWO, SCA, GSA, GA, EPO	TSA, SHO, GWO, GSA, GA, EPO	TSA, SHO, GWO, PSO, MVO, SCA, GA, EPO	TSA, SHO, GWO, PSO, MVO, SCA, GSA, EPO	TSA, SHO, GWO, MVO, SCA, GSA, GA
F_5	2.88E−11	SHO, GWO, PSO, MVO, SCA, GSA, GA, EPO	TSA, PSO, MVO, SCA, GSA, GA, EPO	TSA, SHO, PSO, MVO, SCA, GSA, GA, EPO	TSA, SHO, GWO, MVO, SCA, GSA, GA, EPO	TSA, SHO, GWO, SCA, GSA	TSA, SHO, GWO, PSO, GSA, GA, EPO	TSA, SHO, GWO, PSO, MVO, SCA, GA, EPO	TSA, GWO, PSO, MVO, SCA, GSA, EPO	TSA, SHO, GWO, PSO, MVO GSA, GA
F_6	9.70E−17	SHO, GWO, PSO, MVO, SCA, GSA, GA, EPO	TSA, GWO, PSO, MVO, SCA, GA, EPO	TSA, SHO, PSO, MVO, SCA, GSA, GA, EPO	TSA, SHO, MVO, SCA, GSA, GA, EPO	TSA, SHO, PSO, GSA, GA, EPO	TSA, SHO, MVO, GSA, GA, EPO	TSA, SHO, PSO, SCA, GA, EPO	TSA, SHO, PSO, SCA, GSA, EPO	TSA, SHO, GWO, PSO, MVO, GSA, GA
F_7	6.16E−65	SHO, GWO, PSO, MVO, SCA, GSA	TSA, GWO, PSO, MVO, SCA, GSA, GA, EPO	TSA, SHO, PSO, MVO, SCA, GA, EPO	TSA, SHO, MVO, SCA, GSA, GA, EPO	TSA, SHO, PSO, SCA, GSA, GA, EPO	TSA, SHO, GWO, MVO, GSA	TSA, SHO, GWO, PSO, MVO, SCA, GA, EPO	TSA, SHO, GWO, PSO, MVO, SCA, GSA	TSA, SHO, GWO, PSO, SCA, GSA, GA
F_8	3.53E−11	SHO, GWO, MVO, SCA, GA, EPO	TSA, GWO, MVO, SCA, GSA, EPO	TSA, SHO, PSO, MVO, SCA, GA, EPO	TSA, SHO, MVO, SCA, GSA, GA	TSA, SHO, PSO, GSA, GA, EPO	TSA, SHO, GWO, PSO, GSA, EPO	TSA, SHO, PSO, SCA, GA, EPO	TSA, SHO, GWO, MVO, SCA, GSA, EPO	TSA, SHO, PSO, MVO, SCA
F_9	2.31E−24	SHO, GWO, PSO, MVO, SCA, GSA, GA, EPO	TSA, GWO, MVO, GSA, GA, EPO	TSA, SHO, PSO, MVO, SCA, GSA, GA, EPO	TSA, SHO, SCA, GSA, GA, EPO	TSA, SHO, PSO, SCA, GSA, GA, EPO	TSA, SHO, PSO, GSA, GA, EPO	TSA, SHO, PSO, MVO, GA, EPO	TSA, SHO, GWO, PSO, MVO, SCA, GSA, EPO	TSA, SHO, GWO, PSO, SCA, GSA, GA
F_{10}	6.11E−66	SHO, GWO, PSO, MVO, SCA, GSA, GA, EPO	TSA, GWO, PSO, SCA, GSA, GA, EPO	TSA, SHO, PSO, MVO, SCA, GSA, GA, EPO	TSA, SHO, GWO, GSA	TSA, GWO, PSO, SCA, GSA, GA, EPO	TSA, SHO, GWO, MVO, GA, EPO	TSA, GWO, PSO, MVO, SCA, GA, EPO	TSA, SHO, GWO, SCA	TSA, SHO, GWO, PSO, MVO, SCA, GSA, GA
F_{11}	5.21E−97	SHO, GWO, PSO, MVO, SCA, GSA, EPO	TSA, GWO, PSO, MVO, SCA, GSA, GA, EPO	TSA, SHO, MVO, SCA, GSA, GA, EPO	TSA, SHO, GWO, MVO, SCA, GSA, GA, EPO	TSA, SHO, PSO, GSA, GA, EPO	TSA, SHO, GWO, PSO, MVO, GSA, EPO	TSA, SHO, GWO, MVO, SCA, GA, EPO	TSA, SHO, GWO, PSO, MVO, SCA, EPO	TSA, SHO, GWO, PSO, MVO, GSA, GA
F_{12}	3.98E−71	SHO, GWO, PSO, MVO, SCA, GSA, GA, EPO	TSA, GWO, PSO, SCA, GSA, GA, EPO	TSA, SHO, MVO, SCA, GSA, GA, EPO	TSA, SHO, GWO, MVO, GSA, GA, EPO	TSA, SHO, GWO, SCA, GSA, GA, EPO	TSA, SHO, GWO, GSA, GA, EPO	TSA, SHO, GWO, MVO, SCA, GA, EPO	TSA, SHO, PSO, MVO, SCA, GSA, EPO	TSA, SHO, GWO, PSO, MVO, SCA, GA
F_{13}	3.60E−16	SHO, GWO, PSO, MVO, SCA, GSA, GA, EPO	TSA, GWO, PSO, MVO, SCA, GA, EPO	TSA, SHO, PSO, MVO, SCA, GSA, GA, EPO	TSA, SHO, SCA, GSA, GA, EPO	TSA, SHO, PSO, SCA, GSA, GA, EPO	TSA, SHO, GWO, PSO, GSA, GA, EPO	TSA, SHO, GWO, PSO, MVO, SCA, GA, EPO	TSA, SHO, PSO, MVO, GSA, EPO	TSA, SHO, PSO, MVO, SCA, GA
F_{14}	5.24E−57	SHO, GWO, PSO, MVO, SCA, GSA, EPO	TSA, GWO, PSO, MVO, SCA, GSA, GA, EPO	TSA, SHO, PSO, SCA, GSA	TSA, SHO, MVO, SCA, GSA, GA, EPO	TSA, SHO, PSO, GSA, GA, EPO	TSA, SHO, GWO, GSA, GA, EPO	TSA, GWO, PSO, SCA, GA, EPO	TSA, SHO, GWO, PSO, MVO, GSA, EPO	TSA, SHO, GWO, MVO, SCA
F_{15}	4.19E−17	SHO, GWO, PSO, MVO, SCA, GSA, GA, EPO	TSA, GWO, PSO, MVO, GSA, EPO	TSA, SHO, PSO, SCA, GSA, GA, EPO	TSA, SHO, MVO, SCA, GSA, GA, EPO	TSA, SHO, GWO, SCA, GSA	TSA, SHO, GWO, PSO, MVO, GA, EPO	TSA, SHO, PSO, SCA, GA, EPO	TSA, SHO, GWO, MVO, SCA, GSA	TSA, SHO, GWO, PSO, MVO
F_{16}	4.21E−46	SHO, GWO, PSO, MVO, SCA, GSA, GA, EPO	TSA, GWO, MVO, GSA, GA, EPO	TSA, SHO, PSO, MVO, SCA, GSA, GA, EPO	TSA, SHO, GWO, MVO, SCA, GSA, GA, EPO	TSA, GWO, PSO, SCA, GSA, GA, EPO	TSA, SHO, GWO, GSA	TSA, SHO, GWO, PSO, MVO, SCA	TSA, SHO, GWO, MVO, SCA, GSA, EPO	TSA, SHO, GWO, MVO, SCA, GA
F_{17}	1.11E−59	SHO, GWO, PSO, MVO, SCA, GSA, GA, EPO	TSA, GWO, PSO, MVO, SCA, GSA, GA, EPO	TSA, SHO, PSO, MVO, GSA, GA, EPO	TSA, SHO, GWO, SCA, GSA, GA, EPO	TSA, SHO, PSO, SCA, GA, EPO	TSA, SHO, PSO, GSA, GA, EPO	TSA, SHO, GWO, SCA, GA, EPO	TSA, SHO, GWO, MVO, SCA, GSA, EPO	TSA, SHO, GWO, MVO, SCA, GSA, GA

(*continued on next page*)

Table 12 (*continued*).

F	$p-$ value	TSA	SHO	GWO	PSO	MVO	SCA	GSA	GA	EPO
F_{18}	7.35E−06	SHO, GWO, PSO, MVO, GSA, GA, EPO	TSA, GWO, PSO, MVO, SCA, GA, EPO	TSA, SHO, MVO, SCA, GSA, GA, EPO	TSA, SHO, GSA, GA	TSA, SHO, PSO, SCA, GSA, EPO	TSA, SHO, GWO, PSO, GSA, GA, EPO	TSA, SHO, GWO, PSO, MVO	TSA, SHO, PSO, MVO, SCA, EPO	TSA, SHO, GWO, PSO, MVO, SCA, GSA, GA
F_{19}	5.41E−52	SHO, GWO, PSO, MVO, SCA, GSA, GA, EPO	TSA, GWO, PSO, SCA, GSA, GA, EPO	TSA, SHO, PSO, MVO, SCA, GA, EPO	TSA, SHO, GWO, SCA, GSA, GA, EPO	TSA, SHO, PSO, SCA, GA, EPO	TSA, SHO, PSO, MVO, GA, EPO	TSA, SHO, GWO, PSO, MVO, SCA, EPO	TSA, SHO, PSO, SCA	TSA, GWO, PSO, MVO, SCA, GSA, GA
F_{20}	6.50E−11	SHO, GWO, PSO, MVO, SCA, GSA	TSA, GWO, PSO, MVO, SCA, GSA	TSA, PSO, MVO, SCA, GSA,	TSA, SHO, GWO, MVO, SCA, GSA, GA, EPO	TSA, SHO, GWO, PSO, SCA, GSA, GA, EPO	TSA, SHO, PSO, GSA	TSA, SHO, GWO, MVO, SCA, GA, EPO	TSA, SHO, PSO, MVO, GSA, EPO	TSA, SHO, GWO, PSO, MVO, SCA, GSA, GA
F_{21}	5.10E−03	SHO, GWO, PSO, MVO, SCA, GSA, GA, EPO	TSA, GWO, PSO, MVO, GSA, GA, EPO	TSA, SHO, PSO, MVO, GSA, GA, EPO	TSA, SHO, GWO, MVO, SCA	TSA, SHO, GWO, PSO, SCA, GSA, GA, EPO	TSA, SHO, GWO, PSO, MVO, GSA, GA, EPO	TSA, SHO, PSO, SCA	TSA, SHO, GWO, PSO, MVO, SCA, GSA, EPO	TSA, SHO, GWO, PSO, MVO, SCA, GSA, GA
F_{22}	2.10E−25	SHO, GWO, PSO, MVO, SCA, GSA, GA, EPO	TSA, GWO, PSO, MVO, GSA, GA, EPO	TSA, SHO, PSO, MVO, SCA, GSA, GA, EPO	TSA, MVO, SCA, GA, EPO	TSA, SHO, GWO, PSO, SCA, GSA, GA, EPO	TSA, SHO, PSO, GSA, GA, EPO	TSA, SHO, GWO, PSO, MVO, SCA, GA, EPO	TSA, GWO, PSO, SCA, GSA, EPO	TSA, SHO, PSO, MVO, SCA, GSA, GA
F_{23}	3.75E−42	SHO, GWO, PSO, MVO, SCA, GSA, GA, EPO	TSA, GWO, MVO, SCA, GSA, EPO	TSA, SHO, PSO, MVO, SCA, GSA, GA, EPO	TSA, SHO, GWO, MVO, SCA, GSA, GA, EPO	TSA, SHO, PSO, GSA, GA, EPO	TSA, SHO, GWO, PSO, MVO, GSA, GA	TSA, SHO, MVO, SCA, GA, EPO	TSA, SHO, GWO, MVO, SCA, GSA	TSA, SHO, GWO, PSO, MVO, SCA, GSA, GA
F_{24}	1.52E−43	SHO, GWO, PSO, MVO, SCA, GSA, GA, EPO	TSA, GWO, PSO, MVO, SCA, GSA, GA	TSA, SHO, MVO, GSA, GA, EPO	GWO, MVO, SCA, GSA, GA, EPO	TSA, GWO, PSO, SCA, GSA, GA	TSA, SHO, GWO, PSO, GSA, GA, EPO	SHO, GWO, PSO, MVO, SCA, EPO	TSA, SHO, PSO, MVO, SCA, GSA, EPO	TSA, SHO, GWO, PSO, MVO, SCA, GSA, GA
F_{25}	3.01E−02	SHO, GWO, PSO, MVO, SCA, GSA, GA, EPO	TSA, GWO, MVO, SCA, GSA, GA	TSA, SHO, PSO, MVO, SCA, GA, EPO	TSA, SHO, GWO, MVO, SCA, GSA, EPO	TSA, GWO, SCA, GSA, EPO	TSA, SHO, GWO, PSO, GSA, GA, EPO	TSA, SHO, GWO, PSO, MVO, SCA	TSA, SHO, PSO, SCA, GSA, EPO	TSA, SHO, PSO, SCA, GSA, GA
F_{26}	4.78E−30	SHO, GWO, PSO, MVO, SCA, GSA, GA	TSA, PSO, SCA, GSA, GA, EPO	TSA, SHO, PSO, MVO, SCA	TSA, SHO, MVO, SCA, GSA, GA, EPO	TSA, SHO, GWO, PSO, SCA, GSA, GA, EPO	TSA, SHO, GWO, PSO, MVO, GSA, GA, EPO	TSA, PSO, GA, EPO	TSA, SHO, GWO, PSO, MVO, SCA, GSA, EPO	TSA, SHO, GWO, PSO, MVO, SCA, GSA
F_{27}	9.15E−02	SHO, GWO, PSO, MVO, SCA, GSA, GA, EPO	TSA, GWO, PSO, MVO, SCA, GA, EPO	TSA, SHO, PSO, MVO, SCA, GSA, GA, EPO	TSA, GWO, MVO, GSA, GA, EPO	TSA, SHO, PSO, SCA, GSA, GA, EPO	TSA, SHO, MVO, GSA, GA, EPO	TSA, SHO, GWO, PSO, SCA, GA, EPO	TSA, SHO, GWO, MVO, SCA, GSA, EPO	TSA, SHO, GWO, PSO, MVO, SCA, GSA
F_{28}	2.31E−92	SHO, GWO, PSO, MVO, SCA, GSA, EPO	TSA, MVO, GSA, GA, EPO	TSA, PSO, MVO, SCA, GSA, EPO	TSA, SHO, GWO, MVO, GSA, GA, EPO	TSA, SHO, PSO, GSA, GA, EPO	TSA, GWO, PSO, MVO, GA	TSA, GWO, PSO, MVO, SCA, GA, EPO	TSA, SHO, GWO, MVO, SCA, GSA, EPO	TSA, SHO, GWO, PSO, MVO, SCA, GSA, GA
F_{29}	4.16E−06	SHO, GWO, MVO, SCA, GSA, GA, EPO	TSA, GWO, PSO, MVO, SCA, GSA, GA, EPO	TSA, SHO, MVO, GSA	TSA, SHO, GWO, MVO, SCA, GSA, GA, EPO	TSA, SHO, GWO, PSO, SCA, GSA, GA, EPO	TSA, SHO, MVO, GSA, GA, EPO	TSA, SHO, GWO, PSO, MVO, SCA, GA, EPO	TSA, SHO, PSO, MVO, SCA, GSA	TSA, SHO, PSO, MVO, GSA, GA

Table 13
Comparison of best solution obtained from different algorithms for pressure vessel design problem.

Algorithms	Optimum variables				Optimum cost
	T_s	T_h	R	L	
TSA	0.778090	0.383230	40.315050	200.00000	**5870.9550**
EPO	0.778099	0.383241	40.315121	200.00000	5880.0700
SHO	0.778210	0.384889	40.315040	200.00000	5885.5773
GWO	0.779035	0.384660	40.327793	199.65029	5889.3689
PSO	0.778961	0.384683	40.320913	200.00000	5891.3879
MVO	0.845719	0.418564	43.816270	156.38164	6011.5148
SCA	0.817577	0.417932	41.74939	183.57270	6137.3724
GSA	1.085800	0.949614	49.345231	169.48741	11 550.2976
GA	0.752362	0.399540	40.452514	198.00268	5890.3279

Table 14
Statistical results obtained from different algorithms for pressure vessel design problem.

Algorithms	Best	Mean	Worst	Std. Dev.	Median
TSA	**5870.9550**	**5880.5240**	5882.6580	009.125	**5875.9685**
EPO	5880.0700	5884.1401	5891.3099	024.341	5883.5153
SHO	5885.5773	5887.4441	5892.3207	**002.893**	5886.2282
GWO	5889.3689	5891.5247	5894.6238	013.910	5890.6497
PSO	5891.3879	6531.5032	7394.5879	534.119	6416.1138
MVO	6011.5148	6477.3050	7250.9170	327.007	6397.4805
SCA	6137.3724	6326.7606	6512.3541	126.609	6318.3179
GSA	11 550.2976	23 342.2909	**33 226.2526**	5790.625	24 010.0415
GA	5890.3279	6264.0053	7005.7500	496.128	6112.6899

$$g_7(\vec{z}) = \frac{z_2 z_3}{40} - 1 \le 0,$$
$$g_8(\vec{z}) = \frac{5z_2}{z_1} - 1 \le 0,$$
$$g_9(\vec{z}) = \frac{z_1}{12z_2} - 1 \le 0,$$
$$g_{10}(\vec{z}) = \frac{1.5z_6 + 1.9}{z_4} - 1 \le 0,$$
$$g_{11}(\vec{z}) = \frac{1.1z_7 + 1.9}{z_5} - 1 \le 0,$$

where,

$2.6 \le z_1 \le 3.6,\ 0.7 \le z_2 \le 0.8,\ 17 \le z_3 \le 28,\ 7.3 \le z_4 \le 8.3,$
$7.3 \le z_5 \le 8.3,\ 2.9 \le z_6 \le 3.9,\ 5.0 \le z_7 \le 5.5.$

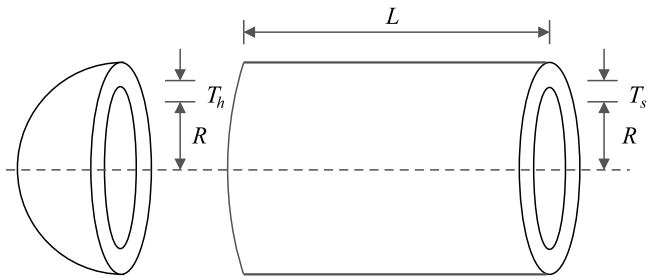

Fig. 11. Schematic view of pressure vessel design problem.

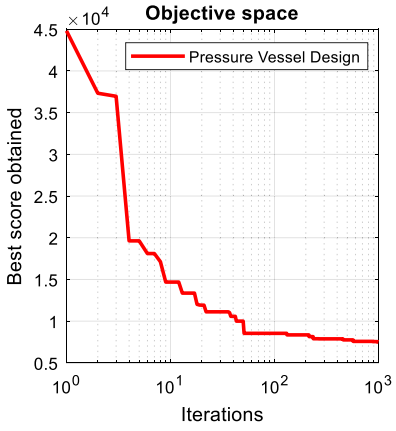

Fig. 12. Convergence analysis of TSA for pressure vessel design problem.

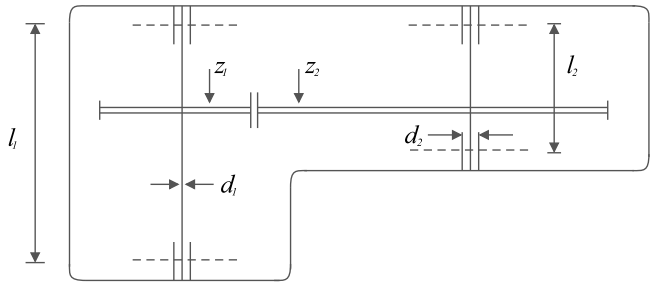

Fig. 13. Schematic view of speed reducer design problem.

Table 15 reveals the obtained optimal solutions by different algorithms on this design problem. The proposed TSA algorithm obtains optimal solution at point $z_{1-7} = (3.50120, 0.7, 17, 7.3, 7.8, 3.33410, 5.26530)$ with corresponding fitness value as $f(z_{1-7}) = 2990.9580$. The statistical results of TSA and other optimization algorithms are tabulated in Table 16.

The results show that TSA is superior than other metaheuristic optimization algorithms. Fig. 14 shows the convergence behavior of the proposed TSA on speed reducer design problem.

5.1.3. Welded beam design problem

The objective of this optimization problem is to minimize the fabrication cost of welded beam as shown in Fig. 15. The optimization constraints of welded beam are shear stress (τ), bending stress (θ) in the beam, buckling load (P_c) on the bar, and end deflection (δ) of the beam. There are four design variables ($z_1 - z_4$) of this problem which are described as:

- h (z_1, thickness of weld)
- l (z_2, length of the clamped bar)
- t (z_3, height of the bar)

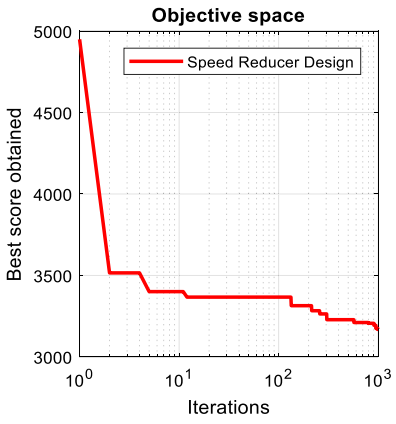

Fig. 14. Convergence analysis of the proposed TSA algorithm for speed reducer design problem.

- b (z_4, thickness of the bar)

The mathematical formulation is described as follows:

$$
\begin{aligned}
&\text{Consider } \vec{z} = [z_1\ z_2\ z_3\ z_4] = [h\ l\ t\ b],\\
&\text{Minimize } f(\vec{z}) = 1.10471 z_1^2 z_2 + 0.04811 z_3 z_4 (14.0 + z_2),\\
&\text{Subject to:}\\
&g_1(\vec{z}) = \tau(\vec{z}) - 13{,}600 \le 0,\\
&g_2(\vec{z}) = \sigma(\vec{z}) - 30{,}000 \le 0,\\
&g_3(\vec{z}) = \delta(\vec{z}) - 0.25 \le 0,\\
&g_4(\vec{z}) = z_1 - z_4 \le 0,\\
&g_5(\vec{z}) = 6000 - P_c(\vec{z}) \le 0,\\
&g_6(\vec{z}) = 0.125 - z_1 \le 0,\\
&g_7(\vec{z}) = 1.10471 z_1^2 + 0.04811 z_3 z_4 (14.0 + z_2) - 5.0 \le 0,
\end{aligned}
\tag{10}
$$

where,

$$
0.1 \le z_1,\ 0.1 \le z_2,\ z_3 \le 10.0,\ z_4 \le 2.0,
$$

$$
\tau(\vec{z}) = \sqrt{(\tau')^2 + (\tau'')^2 + (l\tau'\tau'')/\sqrt{0.25(l^2 + (h+t)^2)}},
$$

$$
\tau' = \frac{6000}{\sqrt{2}hl}, \qquad \sigma(\vec{z}) = \frac{504{,}000}{t^2 b}, \qquad \delta(\vec{z}) = \frac{65{,}856{,}000}{(30 \times 10^6) b t^3},
$$

$$
\tau'' = \frac{6000(14 + 0.5l)\sqrt{0.25(l^2 + (h+t)^2)}}{2[0.707hl(l^2/12 + 0.25(h+t)^2)]},
$$

$$
P_c(\vec{z}) = 64{,}746.022(1 - 0.0282346t) t b^3.
$$

The comparison results between proposed TSA and other metaheuristics is given in Table 17. The proposed TSA obtains optimal solution at point $z_{1-4} = (0.203290, 3.471140, 9.035100, 0.201150)$ with corresponding fitness value equal to $f(z_{1-4}) = 1.721020$. Table 18 shows the statistical comparison of TSA and other competitor algorithms. TSA reveals the superiority than other algorithms in terms of best, mean, and median.

Fig. 16 shows the convergence behavior of best optimal solution obtained from the proposed TSA for welded beam design problem.

5.1.4. Tension/compression spring design problem

The objective of this engineering design problem is to minimize the tension/compression spring weight (see Fig. 17). The constraints are described as follows:

- Shear stress.
- Surge frequency.
- Minimum deflection.

There are three design variables: wire diameter (d), mean coil diameter (D), and the number of active coils (P). The mathematical

Table 15
Comparison of best solution obtained from different algorithms for speed reducer design problem.

Algorithms	Optimum variables							Optimum cost
	b	m	p	l_1	l_2	d_1	d_2	
TSA	3.50120	0.7	17	7.3	7.8	3.33410	5.26530	**2990.9580**
EPO	3.50123	0.7	17	7.3	7.8	3.33421	5.26536	2994.2472
SHO	3.50159	0.7	17	7.3	7.8	3.35127	5.28874	2998.5507
GWO	3.506690	0.7	17	7.380933	7.815726	3.357847	5.286768	3001.288
PSO	3.500019	0.7	17	8.3	7.8	3.352412	5.286715	3005.763
MVO	3.508502	0.7	17	7.392843	7.816034	3.358073	5.286777	3002.928
SCA	3.508755	0.7	17	7.3	7.8	3.461020	5.289213	3030.563
GSA	3.600000	0.7	17	8.3	7.8	3.369658	5.289224	3051.120
GA	3.510253	0.7	17	8.35	7.8	3.362201	5.287723	3067.561

Table 16
Statistical results obtained from different algorithms for speed reducer design problem.

Algorithms	Best	Mean	Worst	Std. Dev.	Median
TSA	**2990.9580**	**2993.010**	2998.425	**1.22408**	**2992.018**
EPO	2994.2472	2997.482	2999.092	1.78091	2996.318
SHO	2998.5507	2999.640	3003.889	1.93193	2999.187
GWO	3001.288	3005.845	3008.752	5.83794	3004.519
PSO	3005.763	3105.252	3211.174	79.6381	3105.252
MVO	3002.928	3028.841	3060.958	13.0186	3027.031
SCA	3030.563	3065.917	3104.779	18.0742	3065.609
GSA	3051.120	3170.334	**3363.873**	92.5726	3156.752
GA	3067.561	3186.523	3313.199	17.1186	3198.187

formulation of this problem is described below:

Consider $\vec{z} = [z_1\ z_2\ z_3] = [d\ D\ P]$,

Minimize $f(\vec{z}) = (z_3 + 2)z_2 z_1^2$, (11)

Subject to:

$$g_1(\vec{z}) = 1 - \frac{z_2^3 z_3}{71785 z_1^4} \leq 0,$$

$$g_2(\vec{z}) = \frac{4z_2^2 - z_1 z_2}{12566(z_2 z_1^3 - z_1^4)} + \frac{1}{5108 z_1^2} \leq 0,$$

$$g_3(\vec{z}) = 1 - \frac{140.45 z_1}{z_2^2 z_3} \leq 0,$$

$$g_4(\vec{z}) = \frac{z_1 + z_2}{1.5} - 1 \leq 0,$$

where,

$0.05 \leq z_1 \leq 2.0,\ 0.25 \leq z_2 \leq 1.3,\ 2.0 \leq z_3 \leq 15.0.$

Table 19 shows the comparison between proposed TSA and other competitor algorithms in terms of design variables values and objective values. TSA generated best solution at design variables z_{1-3} = (0.051080, 0.342890, 12.0890) with an objective function value of $f(z_{1-3})$ = 0.012655520. The results show that TSA is better than the other competitor algorithms on this design problem. The statistical results of tension/compression spring design problem for the reported algorithms are also compared and given in Table 20. It is analyzed from Table 20 that TSA provides better statistical results in terms of best, mean, and median.

Fig. 18 shows the convergence analysis for best optimal design obtained from the proposed TSA.

5.1.5. 25-bar truss design problem

The truss design problem is a popular large-scale optimization problem (Kaveh and Talatahari, 2009a,b) (see Fig. 19). There are 10 nodes and 25 bars cross-sectional members. These are grouped into eight categories.

- Group 1: A_1
- Group 2: A_2, A_3, A_4, A_5
- Group 3: A_6, A_7, A_8, A_9
- Group 4: A_{10}, A_{11}
- Group 5: A_{12}, A_{13}
- Group 6: A_{14}, A_{15}, A_{17}
- Group 7: $A_{18}, A_{19}, A_{20}, A_{21}$
- Group 8: $A_{22}, A_{23}, A_{24}, A_{25}$

The other variables which affects on this problem are as follows:

- $p = 0.0272$ N/cm^3 (0.1 lb/in.^{3})
- E = 68 947 MPa (10 000 Ksi)

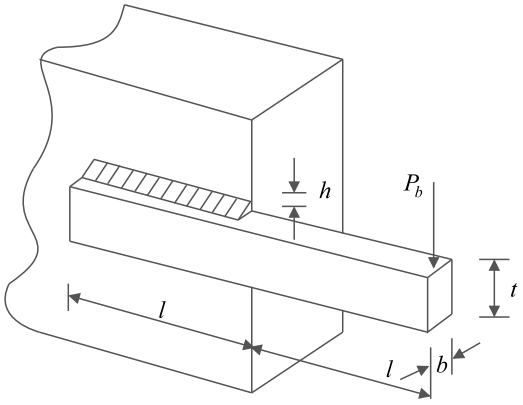

Fig. 15. Schematic view of welded beam problem.

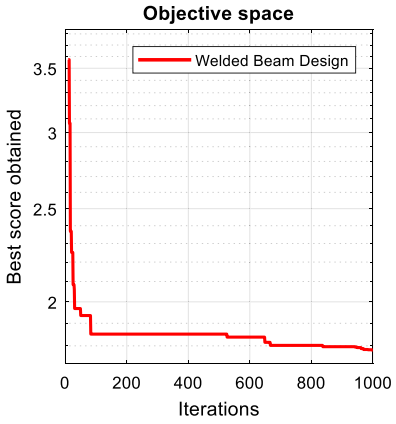

Fig. 16. Convergence analysis of TSA for welded beam design problem.

Fig. 17. Schematic view of tension/compression spring problem.

Table 17
Comparison of best solution obtained from different algorithms for welded beam design problem.

Algorithms	Optimum variables				Optimum cost
	h	l	t	b	
TSA	0.203290	3.471140	9.035100	0.201150	**1.721020**
EPO	0.205411	3.472341	9.035215	0.201153	1.723589
SHO	0.205563	3.474846	9.035799	0.205811	1.725661
GWO	0.205678	3.475403	9.036964	0.206229	1.726995
PSO	0.197411	3.315061	10.00000	0.201395	1.820395
MVO	0.205611	3.472103	9.040931	0.205709	1.725472
SCA	0.204695	3.536291	9.004290	0.210025	1.759173
GSA	0.147098	5.490744	10.00000	0.217725	2.172858
GA	0.164171	4.032541	10.00000	0.223647	1.873971

Table 18
Statistical results obtained from different algorithms for welded beam design problem.

Algorithms	Best	Mean	Worst	Std. Dev.	Median
TSA	**1.721020**	**1.725021**	1.727205	0.003316	**1.724224**
EPO	1.723589	1.725124	1.727211	0.004325	1.724399
SHO	1.725661	1.725828	1.726064	**0.000287**	1.725787
GWO	1.726995	1.727128	1.727564	0.001157	1.727087
PSO	1.820395	2.230310	**3.048231**	0.324525	2.244663
MVO	1.725472	1.729680	1.741651	0.004866	1.727420
SCA	1.759173	1.817657	1.873408	0.027543	1.820128
GSA	2.172858	2.544239	3.003657	0.255859	2.495114
GA	1.873971	2.119240	2.320125	0.034820	2.097048

Table 19
Comparison of best solution obtained from different algorithms for tension/compression spring design problem.

Algorithms	Optimum variables			Optimum cost
	d	D	P	
TSA	0.051080	0.342890	12.0890	**0.012655520**
EPO	0.051087	0.342908	12.0898	0.012656987
SHO	0.051144	0.343751	12.0955	0.012674000
GWO	0.050178	0.341541	12.07349	0.012678321
PSO	0.05000	0.310414	15.0000	0.013192580
MVO	0.05000	0.315956	14.22623	0.012816930
SCA	0.050780	0.334779	12.72269	0.012709667
GSA	0.05000	0.317312	14.22867	0.012873881
GA	0.05010	0.310111	14.0000	0.013036251

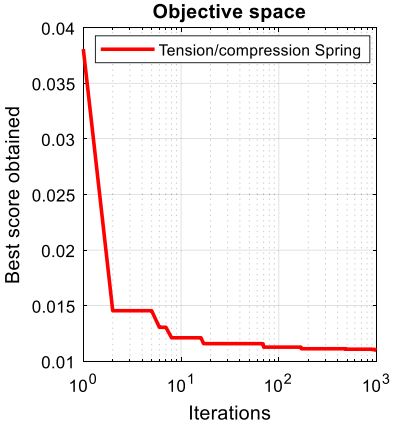

Fig. 18. Convergence analysis of TSA for tension/compression spring design problem.

- Displacement limitation = 0.35 in.
- Maximum displacement = 0.3504 in.
- Design variable set = $\{0.1, 0.2, 0.3, 0.4, 0.5, 0.6, 0.7, 0.8, 0.9, 1.0, 1.1, 1.2, 1.3, 1.4, 1.5, 1.6, 1.7, 1.8, 1.9, 2.0, 2.1, 2.2, 2.3, 2.4, 2.6, 2.8, 3.0, 3.2, 3.4\}$

Table 21 shows the member stress limitations for this problem.

5.1.6. Rolling element bearing design problem

The objective of this design problem is to maximize the dynamic load carrying capacity of a rolling element bearing as shown in Fig. 21. There are 10 decision variables such as pitch diameter (D_m), ball diameter (D_b), number of balls (Z), inner (f_i) and outer (f_o) raceway curvature coefficients, K_{Dmin}, K_{Dmax}, ϵ, e, and ζ (see Fig. 21). The mathematical justification of this problem is described below:

$$\text{Maximize } C_d = \begin{cases} f_c Z^{2/3} D_b^{1.8}, & if\ D \le 25.4 \text{ mm} \\ C_d = 3.647 f_c Z^{2/3} D_b^{1.4}, & if\ D > 25.4 \text{ mm} \end{cases}$$

Subject to:

$$\begin{aligned}
&g_1(\vec{z}) = \frac{\phi_0}{2sin^{-1}(D_b/D_m)} - Z + 1 \le 0,\\
&g_2(\vec{z}) = 2D_b - K_{Dmin}(D-d) \ge 0,\\
&g_3(\vec{z}) = K_{Dmax}(D-d) - 2D_b \ge 0,\\
&g_4(\vec{z}) = \zeta B_w - D_b \le 0,\\
&g_5(\vec{z}) = D_m - 0.5(D+d) \ge 0,\\
&g_6(\vec{z}) = (0.5+e)(D+d) - D_m \ge 0,\\
&g_7(\vec{z}) = 0.5(D - D_m - D_b) - \epsilon D_b \ge 0,\\
&g_8(\vec{z}) = f_i \ge 0.515,\\
&g_9(\vec{z}) = f_o \ge 0.515,
\end{aligned} \tag{12}$$

where,

$$f_c = 37.91\left[1 + \left\{1.04\left(\frac{1-\gamma}{1+\gamma}\right)^{1.72}\left(\frac{f_i(2f_o-1)}{f_o(2f_i-1)}\right)^{0.41}\right\}^{10/3}\right]^{-0.3} \times \left[\frac{\gamma^{0.3}(1-\gamma)^{1.39}}{(1+\gamma)^{1/3}}\right]\left[\frac{2f_i}{2f_i-1}\right]^{0.41}$$

$$x = [\{(D-d)/2 - 3(T/4)\}^2 + \{D/2 - T/4 - D_b\}^2 - \{d/2 + T/4\}^2]$$

$$y = 2\{(D-d)/2 - 3(T/4)\}\{D/2 - T/4 - D_b\}$$

$$\phi_o = 2\pi - 2cos^{-1}\left(\frac{x}{y}\right)$$

$$\gamma = \frac{D_b}{D_m}, \quad f_i = \frac{r_i}{D_b}, \quad f_o = \frac{r_o}{D_b}, \quad T = D - d - 2D_b$$

$$D = 160, \quad d = 90, \quad B_w = 30, \quad r_i = r_o = 11.033$$

$$0.5(D+d) \le D_m \le 0.6(D+d), \quad 0.15(D-d) \le D_b \le 0.45(D-d), \quad 4 \le Z \le 50, \quad 0.515 \le f_i \text{ and } f_o \le 0.6,$$

$$0.4 \le K_{Dmin} \le 0.5, \quad 0.6 \le K_{Dmax} \le 0.7, \quad 0.3 \le e \le 0.4,$$

$$0.02 \le e \le 0.1, \quad 0.6 \le \zeta \le 0.85.$$

Table 24 presents the performance of best obtained optimal solution between proposed and other algorithms. TSA obtains the optimal solution at $z_{1-10} = (125, 21.41750, 10.94109, 0.510, 0.515, 0.4, 0.7, 0.3, 0.02, 0.6)$ with corresponding fitness value as $f(z_{1-10}) = 85\,070.085$. The statistical results for rolling element bearing design problem are tabulated in Table 25. The results reveal that TSA generates the best optimal solution with continuous improvements.

Table 22 shows the loading conditions for 25-bar truss problem. The comparison of best obtained solutions is tabulated in Table 23. It is

Table 20
Statistical results obtained from different algorithms for tension/compression spring design problem.

Algorithms	Best	Mean	Worst	Std. Dev.	Median
TSA	**0.012655520**	**0.012677560**	0.012667890	0.001010	**0.012675990**
EPO	0.012656987	0.012678903	0.012667902	0.001021	0.012676002
SHO	0.012674000	0.012684106	0.012715185	**0.000027**	0.012687293
GWO	0.012678321	0.012697116	0.012720757	0.000041	0.012699686
PSO	0.013192580	0.014817181	**0.017862507**	0.002272	0.013192580
MVO	0.012816930	0.014464372	0.017839737	0.001622	0.014021237
SCA	0.012709667	0.012839637	0.012998448	0.000078	0.012844664
GSA	0.012873881	0.013438871	0.014211731	0.000287	0.013367888
GA	0.013036251	0.014036254	0.016251423	0.002073	0.013002365

Table 21
Member stress limitations for 25-bar truss design problem.

Element group	Compressive stress limitations Ksi (MPa)	Tensile stress limitations Ksi (MPa)
Group 1	35.092 (241.96)	40.0 (275.80)
Group 2	11.590 (79.913)	40.0 (275.80)
Group 3	17.305 (119.31)	40.0 (275.80)
Group 4	35.092 (241.96)	40.0 (275.80)
Group 5	35.092 (241.96)	40.0 (275.80)
Group 6	6.759 (46.603)	40.0 (275.80)
Group 7	6.959 (47.982)	40.0 (275.80)
Group 8	11.082 (76.410)	40.0 (275.80)

analyzed that the proposed TSA is better than other algorithms in terms of best, average, and standard deviation. TSA converges very efficiently towards optimal design of this problem as shown in Fig. 20.

Fig. 22 reveals the convergence behavior of TSA algorithm and it can be seen that TSA is able to achieve best optimal design.

5.2. Unconstrained engineering problem

This subsection describes the displacement of loaded structure design problem to minimize the potential energy.

5.2.1. Displacement of loaded structure design problem

A displacement is a vector which defines the shortest distance between the initial and final position of a given point. The main objective of this unconstrained problem is to minimize the potential energy for reducing the excess load of structure. The loaded structure that should have minimum potential energy ($f(\vec{z})$) is depicted in Fig. 23. The problem can be justified as follows:

$$f(\vec{z}) = \text{Minimize}_{z_1,z_2}\ \pi$$

where,

$$\pi = \frac{1}{2}K_1u_1^2 + \frac{1}{2}K_2u_2^2 - F_zz_1 - F_yz_2 \tag{13}$$

$$K_1 = 8\ \text{N/cm}, K_2 = 1\ \text{N/cm}, F_y = 5\ \text{N}, F_z = 5\ \text{N}$$

$$u_1 = \sqrt{z_1^2 + (10 - z_2^2) - 10}, \quad u_2 = \sqrt{z_1^2 + (10 + z_2^2) - 10}.$$

Table 26 shows the best comparison of optimal solutions obtained from the proposed TSA and other algorithms. TSA achieves best optimum cost at $\pi = 167.2635$. It can be analyzed that TSA is able to minimize the potential energy for loaded structure problem. The statistical results are also given in Table 27. It can be seen that TSA are better than the other metaheuristics in terms of best, mean, and median. Fig. 24 shows the convergence behavior of best optimal design obtained from TSA algorithm.

Overall, TSA is an efficient and effective optimizer for solving both constrained and unconstrained engineering design problems.

6. Conclusion and future scope

In this paper, we presented a bio-inspired based bio-inspired metaheuristic algorithm called Tunicate Swarm Algorithm (TSA). The fundamental inspiration of this algorithm includes the jet propulsion and swarm behaviors of tunicate. The proposed algorithm is experimented on a set of seventy-four benchmark test functions belonging to classical, CEC-2015 and CEC-2017 test suite. The statistical results proved the

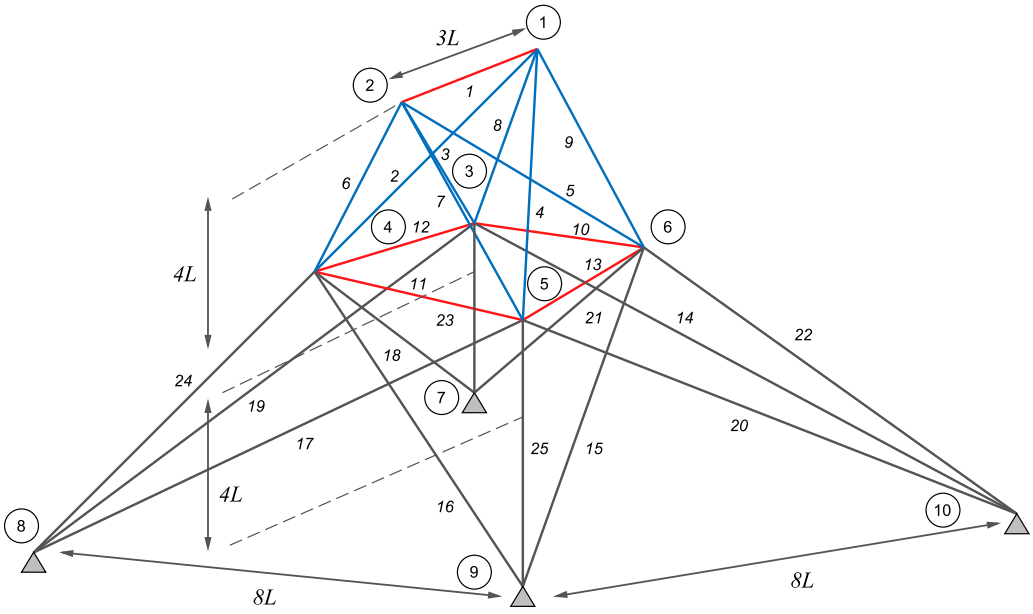

Fig. 19. Schematic view of 25-bar truss problem.

Table 22
Two loading conditions for the 25-bar truss design problem.

Node	Case 1			Case 2		
	$P_x Kips(kN)$	$P_y Kips(kN)$	$P_z Kips(kN)$	$P_x Kips(kN)$	$P_y Kips(kN)$	$P_z Kips(kN)$
1	0.0	20.0 (89)	−5.0 (22.25)	1.0 (4.45)	10.0 (44.5)	−5.0 (22.25)
2	0.0	−20.0 (89)	−5.0 (22.25)	0.0	10.0 (44.5)	−5.0 (22.25)
3	0.0	0.0	0.0	0.5 (2.22)	0.0	0.0
6	0.0	0.0	0.0	0.5 (2.22)	0.0	0.0

Table 23
Statistical results obtained from different algorithms for 25-bar truss design problem.

Groups	TSA	ACO (Bichon, 2004)	PSO (Schutte and Groenwold, 2003)	CSS (Kaveh and Talatahari, 2010)	BB-BC (Kaveh and Talatahari, 2009c)
$A1$	**0.01**	0.01	0.01	0.01	0.01
$A2 - A5$	**1.840**	2.042	2.052	2.003	1.993
$A6 - A9$	**3.001**	3.001	3.001	3.007	3.056
$A10 - A11$	**0.01**	0.01	0.01	0.01	0.01
$A12 - A13$	**0.01**	0.01	0.01	0.01	0.01
$A14 - A17$	**0.651**	0.684	0.684	0.687	0.665
$A18 - A21$	1.620	1.625	**1.616**	1.655	1.642
$A22 - A25$	2.67	2.672	2.673	**2.66**	2.679
Best weight	**544.80**	545.03	545.21	545.10	545.16
Average weight	**545.10**	545.74	546.84	545.58	545.66
Std. dev.	**0.391**	0.94	1.478	0.412	0.491

Table 24
Comparison of best solution obtained from different algorithms for rolling element bearing design problem.

Algorithms	Optimum variables										Opt. cost
	D_m	D_b	Z	f_i	f_o	K_{Dmin}	K_{Dmax}	ε	e	ζ	
TSA	125	21.41750	10.94100	0.510	0.515	0.4	0.7	0.3	0.02	0.6	**85070.080**
EPO	125	21.41890	10.94113	0.515	0.515	0.4	0.7	0.3	0.02	0.6	85 067.983
SHO	125	21.40732	10.93268	0.515	0.515	0.4	0.7	0.3	0.02	0.6	85 054.532
GWO	125.6199	21.35129	10.98781	0.515	0.515	0.5	0.68807	0.300151	0.03254	0.62701	84 807.111
PSO	125	20.75388	11.17342	0.515	0.515000	0.5	0.61503	0.300000	0.05161	0.60000	81 691.202
MVO	125.6002	21.32250	10.97338	0.515	0.515000	0.5	0.68782	0.301348	0.03617	0.61061	84 491.266
SCA	125	21.14834	10.96928	0.515	0.515	0.5	0.7	0.3	0.02778	0.62912	83 431.117
GSA	125	20.85417	11.14989	0.515	0.517746	0.5	0.61827	0.304068	0.02000	0.624638	82 276.941
GA	125	20.77562	11.01247	0.515	0.515000	0.5	0.61397	0.300000	0.05004	0.610001	82 773.982

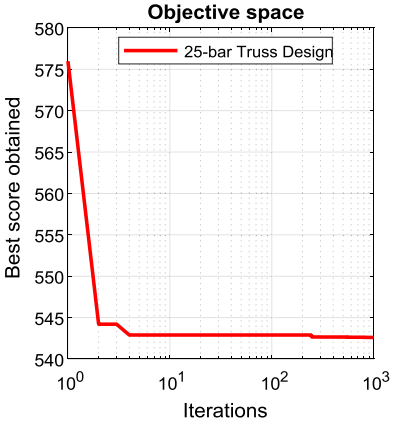

Fig. 20. Convergence analysis of TSA for 25-bar truss design problem.

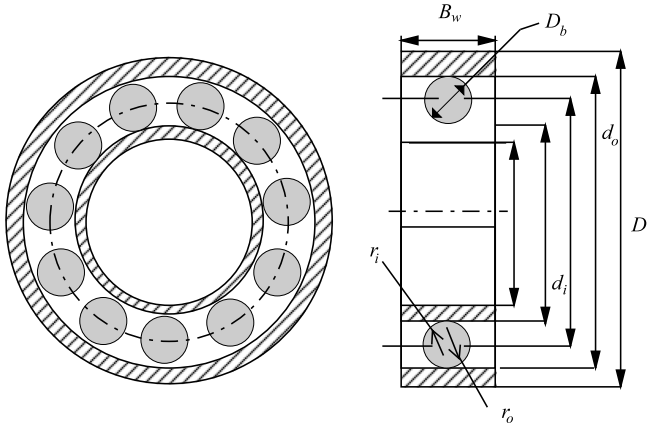

Fig. 21. Schematic view of rolling element bearing problem.

effectiveness of TSA towards attaining global optimal solutions having better convergence in comparison to its rivals.

For CEC-2015 and CEC-2017 benchmark test functions, all the competitor algorithms rarely found the global optimal solutions, contrarily the performance of TSA is found to be accurate and consistent. We also investigated the effect of scalability and sensitivity on efficacy of TSA and the simulation results reveal that the proposed algorithm is less susceptible as compared to other algorithms. In addition, the effectiveness and efficiency of TSA is also demonstrated by applying it on six constrained and one unconstrained engineering design problems. From the experimental outcomes, it can be concluded that the proposed TSA is applicable to real-world case studies with unknown search spaces.

This paper opens several research directions like TSA may be extended in future to solve multi-objective optimization problems. Apart

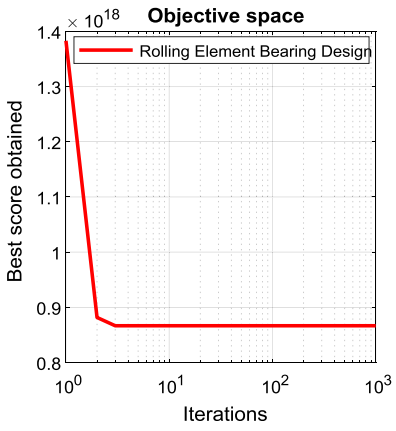

Fig. 22. Convergence analysis of TSA for rolling element bearing design problem.

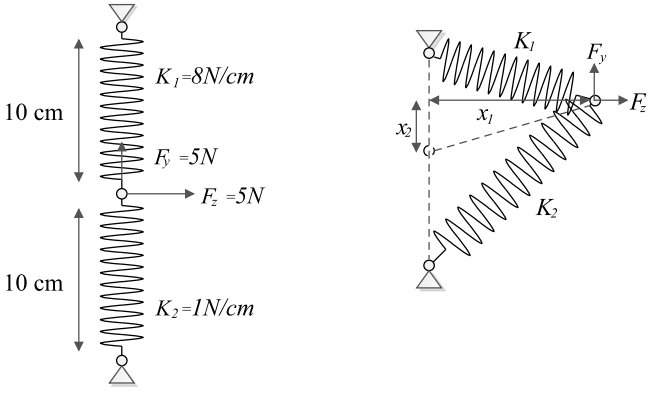

Fig. 23. Schematic view of displacement of loaded structure.

Table 25
Statistical results obtained from different algorithms for rolling element bearing design problem.

Algorithms	Best	Mean	Worst	Std. Dev.	Median
TSA	**85 070.080**	**85 044.951**	86 552.480	1976.21	**85 058.162**
EPO	85 067.983	85 042.352	86 551.599	1877.09	85 056.095
SHO	85 054.532	85 024.858	85 853.876	0186.68	85 040.241
GWO	84 807.111	84 791.613	84 517.923	0137.186	84 960.147
PSO	81 691.202	50 435.017	**32 761.546**	**13 962.150**	42 287.581
MVO	84 491.266	84 353.685	84 100.834	0392.431	84 398.601
SCA	83 431.117	81 005.232	77 992.482	1710.777	81 035.109
GSA	82 276.941	78 002.107	71 043.110	3119.904	78 398.853
GA	82 773.982	81 198.753	80 687.239	1679.367	8439.728

Table 26
Comparison of best solution obtained from different algorithms for displacement of loaded structure problem.

Algorithms	Optimum cost (π)
TSA	**167.0024**
EPO	168.8231
SHO	168.8889
GWO	170.3645
PSO	170.5960
MVO	169.3023
SCA	169.0032
GSA	176.3697
GA	171.3674

from this, the proposal of binary or many objective versions of TSA could be some significant contributions as well.

Table 27
Statistical results obtained from different algorithms for displacement of loaded structure problem.

Algorithms	Best	Mean	Worst	Std. Dev.	Median
TSA	**167.0024**	**169.5302**	176.1111	208.823	**168.5217**
EPO	168.8231	170.1309	**230.9721**	211.861	169.4214
SHO	168.8889	170.3659	173.6357	**023.697**	169.6710
GWO	170.3645	171.3694	174.3970	196.037	173.3694
PSO	170.5960	174.6354	175.3602	236.036	173.9634
MVO	169.3023	171.0034	174.3047	202.753	170.0032
SCA	169.0032	171.7530	174.4527	129.047	170.3647
GSA	176.3697	178.7521	179.5637	113.037	174.367
GA	171.3674	172.0374	174.0098	212.703	172.0097

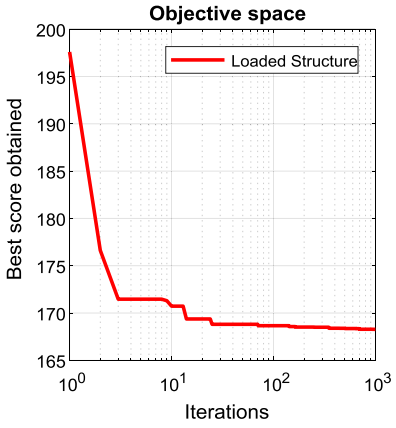

Fig. 24. Convergence analysis of TSA for displacement of loaded structure problem.

CRediT authorship contribution statement

Satnam Kaur conceptualize the data and write the paper, Lalit K. Awasthi proposed the methodology, A.L. Sangal simulate the software, and Gaurav Dhiman investigate the proposed algorithm.

Acknowledgment

The corresponding author, **Dr. Gaurav Dhiman**, would like to thanks to the goddess **SHRI MATA VAISHNO DEVI** for her divine blessings on him.

Appendix. Unimodal, multimodal, and fixed-dimension multimodal benchmark test functions

A.1. Unimodal benchmark test functions

A.1.1. Sphere model

$$F_1(z) = \sum_{i=1}^{30} z_i^2$$

$$-100 \le z_i \le 100, \quad f_{min} = 0, \quad Dim = 30$$

A.1.2. Schwefel's problem 2.22

$$F_2(z) = \sum_{i=1}^{30} |z_i| + \prod_{i=1}^{30} |z_i|$$

$$-10 \le z_i \le 10, \quad f_{min} = 0, \quad Dim = 30$$

Table 28
Shekel's Foxholes function F_{14}.

$(a_{ij}, i = 1, 2$ and $j = 1, 2, \ldots, 25)$								
$i \backslash j$	1	2	3	4	5	6	...	25
1	−32	−16	0	16	32	−32	...	32
2	−32	−32	−32	−32	−32	−16	...	32

Table 29
Hartman function F_{19}.

i	$(a_{ij}, j = 1, 2, 3)$			c_i	$(p_{ij}, j = 1, 2, 3)$		
1	3	10	30	1	0.3689	0.1170	0.2673
2	0.1	10	35	1.2	0.4699	0.4387	0.7470
3	3	10	30	3	0.1091	0.8732	0.5547
4	0.1	10	35	3.2	0.038150	0.5743	0.8828

Table 30
Shekel Foxholes functions F_{21}, F_{22}, F_{23}.

i	$(a_{ij}, j = 1, 2, 3, 4)$				c_i
1	4	4	4	4	0.1
2	1	1	1	1	0.2
3	8	8	8	8	0.2
4	6	6	6	6	0.4
5	3	7	3	7	0.4
6	2	9	2	9	0.6
7	5	5	3	3	0.3
8	8	1	8	1	0.7
9	6	2	6	2	0.5
10	7	3.6	7	3.6	0.5

A.1.3. Schwefel's problem 1.2

$$F_3(z) = \sum_{i=1}^{30}\left(\sum_{j=1}^{i} z_j\right)^2$$

$$-100 \le z_i \le 100, \quad f_{min} = 0, \quad Dim = 30$$

A.1.4. Schwefel's problem 2.21

$$F_4(z) = max_i\{|z_i|, 1 \le i \le 30\}$$

$$-100 \le z_i \le 100, \quad f_{min} = 0, \quad Dim = 30$$

A.1.5. Generalized Rosenbrock's function

$$F_5(z) = \sum_{i=1}^{29}[100(z_{i+1} - z_i^2)^2 + (z_i - 1)^2]$$

$$-30 \le z_i \le 30, \quad f_{min} = 0, \quad Dim = 30$$

A.1.6. Step function

$$F_6(z) = \sum_{i=1}^{30}(\lfloor z_i + 0.5 \rfloor)^2$$

$$-100 \le z_i \le 100, \quad f_{min} = 0, \quad Dim = 30$$

A.1.7. Quartic function

$$F_7(z) = \sum_{i=1}^{30} i z_i^4 + random[0, 1]$$

$$-1.28 \le z_i \le 1.28, \quad f_{min} = 0, \quad Dim = 30$$

A.2. Multimodal benchmark test functions

A.2.1. Generalized Schwefel's problem 2.26

$$F_8(z) = \sum_{i=1}^{30} -z_i sin(\sqrt{|z_i|})$$

$$-500 \le z_i \le 500, \quad f_{min} = -12\,569.5, \quad Dim = 30$$

A.2.2. Generalized Rastrigin's function

$$F_9(z) = \sum_{i=1}^{30}[z_i^2 - 10cos(2\pi z_i) + 10]$$

$$-5.12 \le z_i \le 5.12, \quad f_{min} = 0, \quad Dim = 30$$

A.2.3. Ackley's function

$$F_{10}(z) = -20exp\left(-0.2\sqrt{\frac{1}{30}\sum_{i=1}^{30} z_i^2}\right) - exp\left(\frac{1}{30}\sum_{i=1}^{30} cos(2\pi z_i)\right) + 20 + e$$

$$-32 \le z_i \le 32, \quad f_{min} = 0, \quad Dim = 30$$

A.2.4. Generalized Griewank function

$$F_{11}(z) = \frac{1}{4000}\sum_{i=1}^{30} z_i^2 - \prod_{i=1}^{30} cos\left(\frac{z_i}{\sqrt{i}}\right) + 1$$

$$-600 \le z_i \le 600, \quad f_{min} = 0, \quad Dim = 30$$

A.2.5. Generalized Penalized functions

- $$F_{12}(z) = \frac{\pi}{30}\{10sin(\pi x_1) + \sum_{i=1}^{29}(x_i - 1)^2[1 + 10sin^2(\pi x_{i+1})] + (x_n - 1)^2\} + \sum_{i=1}^{30} u(z_i, 10, 100, 4)$$
$$-50 \le z_i \le 50, \quad f_{min} = 0, \quad Dim = 30$$

- $$F_{13}(z) = 0.1\{sin^2(3\pi z_1) + \sum_{i=1}^{29}(z_i - 1)^2[1 + sin^2(3\pi z_i + 1)] + (z_n - 1)^2 \times [1 + sin^2(2\pi z_{30})]\} + \sum_{i=1}^{N} u(z_i, 5, 100, 4)$$
$$-50 \le z_i \le 50, \quad f_{min} = 0, \quad Dim = 30$$

where, $x_i = 1 + \frac{z_i + 1}{4}$

$$u(z_i, a, k, m) = \begin{cases} k(z_i - a)^m & z_i > a \\ 0 & -a < z_i < a \\ k(-z_i - a)^m & z_i < -a \end{cases}$$

A.3. Fixed-dimension multimodal benchmark test functions

A.3.1. Shekel's Foxholes function

See Table 28.

$$F_{14}(z) = \left(\frac{1}{500} + \sum_{j=1}^{25}\frac{1}{j + \sum_{i=1}^{2}(z_i - a_{ij})^6}\right)^{-1}$$

$$-65.536 \le z_i \le 65.536, \quad f_{min} \approx 1, \quad Dim = 2$$

Table 31
Hartman function F_{20}.

i	$(a_{ij}, j = 1, 2, \dots, 6)$						c_i	$(p_{ij}, j = 1, 2, \dots, 6)$					
1	10	3	17	3.5	1.7	8	1	0.1312	0.1696	0.5569	0.0124	0.8283	0.5886
2	0.05	10	17	0.1	8	14	1.2	0.2329	0.4135	0.8307	0.3736	0.1004	0.9991
3	3	3.5	1.7	10	17	8	3	0.2348	0.1415	0.3522	0.2883	0.3047	0.6650
4	17	8	0.05	10	0.1	14	3.2	0.4047	0.8828	0.8732	0.5743	0.1091	0.0381

Table A.1
Composite benchmark test functions.

Functions	Dim	Range	f_{min}
$F_{24}(CF1)$: $f_1, f_2, f_3, \dots, f_{10}$ = Sphere function $[\alpha_1, \alpha_2, \alpha_3, \dots, \alpha_{10}] = [1, 1, 1, \dots, 1]$ $[\beta_1, \beta_2, \beta_3, \dots, \beta_{10}] = [5/100, 5/100, 5/100, \dots, 5/100]$	10	$[-5, 5]$	0
$F_{25}(CF2)$: $f_1, f_2, f_3, \dots, f_{10}$ = Griewank's Function $[\alpha_1, \alpha_2, \alpha_3, \dots, \alpha_{10}] = [1, 1, 1, \dots, 1]$ $[\beta_1, \beta_2, \beta_3, \dots, \beta_{10}] = [5/100, 5/100, 5/100, \dots, 5/100]$	10	$[-5, 5]$	0
$F_{26}(CF3)$: f_1, f_2 = Ackley's Function $f_1, f_2, f_3, \dots, f_{10}$ = Griewank's Function $[\alpha_1, \alpha_2, \alpha_3, \dots, \alpha_{10}] = [1, 1, 1, \dots, 1]$ $[\beta_1, \beta_2, \beta_3, \dots, \beta_{10}] = [1, 1, 1, \dots, 1]$	10	$[-5, 5]$	0
$F_{27}(CF4)$: f_1, f_2 = Ackley's Function f_3, f_4 = Rastrigin's Function f_5, f_6 = Weierstras's Function f_7, f_8 = Griewank's Function f_9, f_{10} = Sphere Function $[\alpha_1, \alpha_2, \alpha_3, \dots, \alpha_{10}] = [1, 1, 1, \dots, 1]$ $[\beta_1, \beta_2, \beta_3, \dots, \beta_{10}] = [5/32, 5/32, 1, 1, 5/0.5, 5/0.5, 5/100, 5/100, 5/100, 5/100]$	10	$[-5, 5]$	0
$F_{28}(CF5)$: f_1, f_2 = Rastrigin's Function f_3, f_4 = Weierstras's Function f_5, f_6 = Griewank's Function f_7, f_8 = Ackley's Function f_9, f_{10} = Sphere Function $[\alpha_1, \alpha_2, \alpha_3, \dots, \alpha_{10}] = [1, 1, 1, \dots, 1]$ $[\beta_1, \beta_2, \beta_3, \dots, \beta_{10}] = [1/5, 1/5, 5/0.5, 5/0.5, 5/100, 5/100, 5/32, 5/32, 5/100, 5/100]$	10	$[-5, 5]$	0
$F_{29}(CF6)$: f_1, f_2 = Rastrigin's Function f_3, f_4 = Weierstras's Function f_5, f_6 = Griewank's Function f_7, f_8 = Ackley's Function f_9, f_{10} = Sphere Function $[\alpha_1, \alpha_2, \alpha_3, \dots, \alpha_{10}] = [0.1, 0.2, 0.3, 0.4, 0.5, 0.6, 0.7, 0.8, 0.9, 1]$ $[\beta_1, \beta_2, \beta_3, \dots, \beta_{10}] =$ $[0.1 * 1/5, 0.2 * 1/5, 0.3 * 5/0.5, 0.4 * 5/0.5, 0.5 * 5/100, 0.6 * 5/100, 0.7 * 5/32, 0.8 * 5/32, 0.9 * 5/100, 1 * 5/100]$	10	$[-5, 5]$	0

A.3.2. Kowalik's function

$$F_{15}(z) = \sum_{i=1}^{11}\left[a_i - \frac{z_1(b_i^2 + b_i z_2)}{b_i^2 + b_i z_3 + z_4}\right]^2$$

$$-5 \le z_i \le 5, \quad f_{min} \approx 0.0003075, \quad Dim = 4$$

A.3.3. Six-Hump Camel-Back function

$$F_{16}(z) = 4z_1^2 - 2.1z_1^4 + \frac{1}{3}z_1^6 + z_1 z_2 - 4z_2^2 + 4z_2^4$$

$$-5 \le z_i \le 5, \quad f_{min} = -1.0316285, \quad Dim = 2$$

A.3.4. Branin function

$$F_{17}(z) = \left(z_2 - \frac{5.1}{4\pi^2}z_1^2 + \frac{5}{\pi}z_1 - 6\right)^2 + 10\left(1 - \frac{1}{8\pi}\right)cos z_1 + 10$$

$$-5 \le z_1 \le 10, \quad 0 \le z_2 \le 15, \quad f_{min} = 0.398, \quad Dim = 2$$

A.3.5. Goldstein–price function

$$\begin{aligned} F_{18}(z) = {} & [1 + (z_1 + z_2 + 1)^2(19 - 14z_1 + 3z_1^2 - 14z_2 + 6z_1 z_2 + 3z_2^2)] \\ & \times [30 + (2z_1 - 3z_2)^2 \times (18 - 32z_1 + 12z_1^2 + 48z_2 \\ & - 36z_1 z_2 + 27z_2^2)] \end{aligned}$$

$$-2 \le z_i \le 2, \quad f_{min} = 3, \quad Dim = 2$$

A.3.6. Hartman's family

- $F_{19}(z) = -\sum_{i=1}^{4} c_i exp(-\sum_{j=1}^{3} a_{ij}(z_j - p_{ij})^2)$ $0 \le z_j \le 1$, $f_{min} = -3.86$, $Dim = 3$
- $F_{20}(z) = -\sum_{i=1}^{4} c_i exp(-\sum_{j=1}^{6} a_{ij}(z_j - p_{ij})^2)$ $0 \le z_j \le 1$, $f_{min} = -3.32$, $Dim = 6$ (see Table 29).

A.3.7. Shekel's Foxholes function

- $F_{21}(z) = -\sum_{i=1}^{5}[(X - a_i)(X - a_i)^T + c_i]^{-1}$ $0 \le z_i \le 10$, $f_{min} = -10.1532$, $Dim = 4$
- $F_{22}(z) = -\sum_{i=1}^{7}[(X - a_i)(X - a_i)^T + c_i]^{-1}$ $0 \le z_i \le 10$, $f_{min} = -10.4028$, $Dim = 4$
- $F_{23}(z) = -\sum_{i=1}^{10}[(X - a_i)(X - a_i)^T + c_i]^{-1}$ $0 \le z_i \le 10$, $f_{min} = -10.536$, $Dim = 4$ (see Tables 30 and 31).

Table A.2
IEEE CEC-2015 benchmark test functions.

No.	Functions	Related basic functions	Dim	f_{min}
$CEC-1$	Rotated Bent Cigar Function	Bent Cigar Function	30	100
$CEC-2$	Rotated Discus Function	Discus Function	30	200
$CEC-3$	Shifted and Rotated Weierstrass Function	Weierstrass Function	30	300
$CEC-4$	Shifted and Rotated Schwefel's Function	Schwefel's Function	30	400
$CEC-5$	Shifted and Rotated Katsuura Function	Katsuura Function	30	500
$CEC-6$	Shifted and Rotated HappyCat Function	HappyCat Function	30	600
$CEC-7$	Shifted and Rotated HGBat Function	HGBat Function	30	700
$CEC-8$	Shifted and Rotated Expanded Griewank's plus Rosenbrock's Function	Griewank's Function Rosenbrock's Function	30	800
$CEC-9$	Shifted and Rotated Expanded Scaffer's F6 Function	Expanded Scaffer's F6 Function	30	900
$CEC-10$	Hybrid Function 1 ($N=3$)	Schwefel's Function Rastrigin's Function High Conditioned Elliptic Function	30	1000
$CEC-11$	Hybrid Function 2 ($N=4$)	Griewank's Function Weierstrass Function Rosenbrock's Function Scaffer's F6 Function	30	1100
$CEC-12$	Hybrid Function 3 ($N=5$)	Katsuura Function HappyCat Function Expanded Griewank's plus Rosenbrock's Function Schwefel's Function Ackley's Function	30	1200
$CEC-13$	Composition Function 1 ($N=5$)	Rosenbrock's Function High Conditioned Elliptic Function Bent Cigar Function Discus Function High Conditioned Elliptic Function	30	1300
$CEC-14$	Composition Function 2 ($N=3$)	Schwefel's Function Rastrigin's Function High Conditioned Elliptic Function	30	1400
$CEC-15$	Composition Function 3 ($N=5$)	HGBat Function Rastrigin's Function Schwefel's Function Weierstrass Function High Conditioned Elliptic Function	30	1500

A.4. Basic composite benchmark test functions

A.4.1. Weierstrass function

$$F(z)=\sum_{i=1}^{30}\Big(\sum_{k=0}^{20}[0.5^k cos(2\pi 3^k(z_i+0.5))]\Big)-30\sum_{k=0}^{20}[0.5^k cos(2\pi 3^k\times 0.5)]$$

Note that the Sphere, Rastrigin's, Griewank's, and Ackley's functions in composite benchmark suite are same as above mentioned F_1, F_9, F_{11}, and F_{10} benchmark test functions.

A.5. Basic CEC-2015 benchmark test functions

A.5.1. Bent Cigar function

$$F(z)=z_1^2+10^6\sum_{i=2}^{30}z_i^2$$

A.5.2. Discus function

$$F(z)=10^6 z_1^2+\sum_{i=2}^{30}z_i^2$$

A.5.3. Modified Schwefel's function

$$F(z)=418.9829\times 30-\sum_{i=1}^{30}g(y_i),\quad y_i=z_i+4.209687462275036e+002$$

$$g(y_i)=\begin{cases} y_i sin(|y_i|^{1/2}) \\ \quad where, if\ |y_i|\le 500, \\ (500-mod(y_i,500))sin(\sqrt{|500-mod(y_i,500)|})-\dfrac{(y_i-500)^2}{10000\times 30} \\ \quad where, if\ y_i>500, \\ (mod(|y_i|,500)-500)sin(\sqrt{|mod(|y_i|,500)-500|})-\dfrac{(y_i+500)^2}{10000\times 30} \\ \quad where, if\ y_i<-500 \end{cases}$$

A.5.4. Katsuura function

$$F(z)=\frac{10}{30^2}\prod_{i=1}^{30}\Big(1+i\sum_{j=1}^{32}\frac{|2^j z_i-round(2^j z_i)|}{2^j}\Big)^{\frac{10}{30^{1.2}}}-\frac{10}{30^2}$$

A.5.5. HappyCat function

$$F(z)=\Big|\sum_{i=1}^{30}z_i^2-30\Big|^{1/4}+(0.5\sum_{i=1}^{30}z_i^2+\sum_{i=1}^{30}z_i)/30+0.5$$

A.5.6. HGBat function

$$F(z)=\Big|(\sum_{i=1}^{30}z_i^2)^2-(\sum_{i=1}^{30}z_i)^2\Big|^{1/2}+(0.5\sum_{i=1}^{30}z_i^2+\sum_{i=1}^{30}z_i)/30+0.5$$

A.5.7. Expanded Griewank's plus Rosenbrock's function

$$F(z)=F_{39}(F_{38}(z_1,z_2))+F_{39}(F_{38}(z_2,z_3))+\cdots+F_{39}(F_{38}(z_{30},z_1))$$

Table A.3
IEEE CEC-2017 benchmark test functions.

No.	Functions	f_{min}
$C-1$	Shifted and Rotated Bent Cigar Function	100
$C-2$	Shifted and Rotated Sum of Different Power Function	200
$C-3$	Shifted and Rotated Zakharov Function	300
$C-4$	Shifted and Rotated Rosenbrock's Function	400
$C-5$	Shifted and Rotated Rastrigin's Function	500
$C-6$	Shifted and Rotated Expanded Scaffer's Function	600
$C-7$	Shifted and Rotated Lunacek Bi_Rastrigin Function	700
$C-8$	Shifted and Rotated Non-Continuous Rastrigin's Function	800
$C-9$	Shifted and Rotated Levy Function	900
$C-10$	Shifted and Rotated Schwefel's Function	1000
$C-11$	Hybrid Function 1 ($N=3$)	1100
$C-12$	Hybrid Function 2 ($N=3$)	1200
$C-13$	Hybrid Function 3 ($N=3$)	1300
$C-14$	Hybrid Function 4 ($N=4$)	1400
$C-15$	Hybrid Function 5 ($N=4$)	1500
$C-16$	Hybrid Function 6 ($N=4$)	1600
$C-17$	Hybrid Function 6 ($N=5$)	1700
$C-18$	Hybrid Function 6 ($N=5$)	1800
$C-19$	Hybrid Function 6 ($N=5$)	1900
$C-20$	Hybrid Function 6 ($N=6$)	2000
$C-21$	Composition Function 1 ($N=3$)	2100
$C-22$	Composition Function 2 ($N=3$)	2200
$C-23$	Composition Function 3 ($N=4$)	2300
$C-24$	Composition Function 4 ($N=4$)	2400
$C-25$	Composition Function 5 ($N=5$)	2500
$C-26$	Composition Function 6 ($N=5$)	2600
$C-27$	Composition Function 7 ($N=6$)	2700
$C-28$	Composition Function 8 ($N=6$)	2800
$C-29$	Composition Function 9 ($N=3$)	2900
$C-30$	Composition Function 10 ($N=3$)	3000

A.5.8. Expanded Scaffer's $F6$ function

Scaffer's $F6$ Function:

$$g(z,x) = 0.5 + \frac{(sin^2(\sqrt{z^2+x^2}) - 0.5)}{(1+0.001(z^2+x^2))^2}$$

$$F(z) = g(z_1,z_2) + g(z_2,z_3) + \cdots + g(z_{30},z_1)$$

A.5.9. High conditioned Elliptic function

$$F(z) = \sum_{i=1}^{30} (10^6)\frac{i-1}{30-1} z_i^2$$

Note that the Weierstrass, Rosenbrock's, Griewank's, Rastrigin's, and Ackley's functions in CEC-2015 benchmark test suite are same as above mentioned $Weierstrass$, F_5, F_{11}, F_9, and F_{10} benchmark test functions.

A.6. Composite benchmark functions

The detailed description of six well-known composite benchmark test functions ($F_{24} - F_{29}$) are mentioned in Table A.1.

A.7. CEC-2015 benchmark test functions

The detailed description of fifteen well-known CEC-2015 benchmark test functions ($CEC1 - CEC15$) are mentioned in Table A.2.

A.8. CEC-2017 benchmark test functions

The detailed description of fifteen well-known CEC-2017 benchmark test functions ($C1 - C30$) are mentioned in Table A.3.

References

Alba, E., Dorronsoro, B., 2005. The exploration/exploitation tradeoff in dynamic cellular genetic algorithms. IEEE Trans. Evol. Comput. 9 (2), 126–142.

Awad, N., Ali, M., Liang, J., Qu, B., Suganthan, P., 2016. Problem Definitions and Evaluation Criteria for the Cec 2017 Special Session and Competition on Single Objective Bound Constrained Real-Parameter Numerical Optimization. Technical Report, Nanyang Technological University Singapore.

Berrill, J., 1950. The Tuniccafa. The Royal Society, London.

Bichon, C.V.C.B.J., 2004. Design of space trusses using ant colony optimization. J. Struct. Eng. 130 (5), 741–751.

Brest, J., Maučec, M.S., Bošković, B., 2017. Single objective real-parameter optimization: algorithm jso. In: 2017 IEEE Congress on Evolutionary Computation (CEC). IEEE, pp. 1311–1318.

Chandrawat, R.K., Kumar, R., Garg, B., Dhiman, G., Kumar, S., 2017. An analysis of modeling and optimization production cost through fuzzy linear programming problem with symmetric and right angle triangular fuzzy number. In: Proceedings of Sixth International Conference on Soft Computing for Problem Solving. Springer, pp. 197–211.

Chen, Q., Liu, B., Zhang, Q., Liang, J., Suganthan, P., Qu, B., 2014. Problem Definitions and Evaluation Criteria for Cec 2015 Special Session on Bound Constrained Single-Objective Computationally Expensive Numerical Optimization. Technical Report, Computational Intelligence Laboratory, Zhengzhou University, Zhengzhou, China and Technical Report, Nanyang Technological University.

Davenport, J., Balazs, G.H., 1991. 'fiery bodies' - are pyrosomas an important component of the diet of leatherback turtles?. Br. Herpetol. Soc. Bull. 37, 33–38.

Dehghani, M., Montazeri, Z., Malik, O.P., Dhiman, G., Kumar, V., 2019. Bosa: Binary orientation search algorithm. Int. J. Innov. Technol. Explor. Eng. 9, 5306–5310.

Dhiman, G., 2019a. Esa: a hybrid bio-inspired metaheuristic optimization approach for engineering problems. Eng. Comput. 1–31.

Dhiman, G., 2019b. Multi-Objective Metaheuristic Approaches for Data Clustering in Engineering Application (S) (Ph.D. dissertation).

Dhiman, G., 2019c. Moshepo: a hybrid multi-objective approach to solve economic load dispatch and micro grid problems. Appl. Intell. 1–19.

Dhiman, G., Guo, S., Kaur, S., 2018. Ed-sho: A framework for solving nonlinear economic load power dispatch problem using spotted hyena optimizer. Modern Phys. Lett. A 33 (40).

Dhiman, G., Kaur, A., 2017. Spotted hyena optimizer for solving engineering design problems. In: 2017 International Conference on Machine Learning and Data Science (MLDS). IEEE, pp. 114–119.

Dhiman, G., Kaur, A., 2018. Optimizing the design of airfoil and optical buffer problems using spotted hyena optimizer. Designs 2 (3), 28.

Dhiman, G., Kaur, A., 2019a. A hybrid algorithm based on particle swarm and spotted hyena optimizer for global optimization. In: Soft Computing for Problem Solving. Springer, pp. 599–615.

Dhiman, G., Kaur, A., 2019b. Stoa: A bio-inspired based optimization algorithm for industrial engineering problems. Eng. Appl. Artif. Intell. 82, 148–174.

Dhiman, G., Kumar, V., 2017. Spotted hyena optimizer: A novel bio-inspired based metaheuristic technique for engineering applications. Adv. Eng. Softw. 114, 48–70.

Dhiman, G., Kumar, V., 2018a. Astrophysics inspired multi-objective approach for automatic clustering and feature selection in real-life environment. Mod. Phys. Lett. B 32 (31).

Dhiman, G., Kumar, V., 2018b. Emperor penguin optimizer: A bio-inspired algorithm for engineering problems. Knowl.-Based Syst. 159, 20–50, [Online]. Available: http://www.sciencedirect.com/science/article/pii/S095070511830296X.

Dhiman, G., Kumar, V., 2018c. Multi-objective spotted hyena optimizer: A multi-objective optimization algorithm for engineering problems. Knowl.-Based Syst. 150, 175–197.

Dhiman, G., Kumar, V., 2019a. Knrvea: A hybrid evolutionary algorithm based on knee points and reference vector adaptation strategies for many-objective optimization. Appl. Intell. 49 (7), 2434–2460.

Dhiman, G., Kumar, V., 2019b. Seagull optimization algorithm: Theory and its applications for large-scale industrial engineering problems. Knowl.-Based Syst. 165, 169–196.

Dhiman, G., Kumar, V., 2019c. Spotted hyena optimizer for solving complex and non-linear constrained engineering problems. In: Harmony Search and Nature Inspired Optimization Algorithms. Springer, pp. 857–867.

Dhiman, G., Singh, P., Kaur, H., Maini, R., 2019. Dhiman: A novel algorithm for economic d ispatch problem based on optimization met h od us i ng m onte carlo simulation and a strophysics co n cepts. Modern Phys. Lett. A 34 (04).

Digalakis, J., Margaritis, K., 2001. On benchmarking functions for genetic algorithms. Int. J. Comput. Math. 77 (4), 481–506.

Dorigo, M., Birattari, M., Stutzle, T., 2006. Ant colony optimization - artificial ants as a computational intelligence technique. IEEE Comput. Intell. Mag. 1, 28–39.

Gandomi, A.H., Yang, X.-S., 2011. Benchmark Problems in Structural Optimization. Springer Berlin Heidelberg, pp. 259–281.

Garg, M., Dhiman, G., 2020. Deep convolution neural network approach for defect inspection of textured surfaces. J. Inst. Electron. Comput. 2, 28–38.

Holland, J.H., 1992. Genetic algorithms. Sci. Amer. 267 (1), 66–72.

Kannan, B., Kramer, S.N., 1994. An augmented lagrange multiplier based method for mixed integer discrete continuous optimization and its applications to mechanical design. J. Mech. Des. 116 (2), 405–411.

Kaur, A., Dhiman, G., 2019. A review on search-based tools and techniques to identify bad code smells in object-oriented systems. In: Harmony Search and Nature Inspired Optimization Algorithms. Springer, pp. 909–921.

Kaur, A., Kaur, S., Dhiman, G., 2018. A quantum method for dynamic nonlinear programming technique using schrödinger equation and monte carlo approach. Mod. Phys. Lett. B 32 (30).

Kaveh, A., Talatahari, S., 2009a. A particle swarm ant colony optimization for truss structures with discrete variables. J. Construct. Steel Res. 65 (8–9), 1558–1568.

Kaveh, A., Talatahari, S., 2009b. Particle swarm optimizer ant colony strategy and harmony search scheme hybridized for optimization of truss structures. Comput. Struct. 87 (5–6), 267–283.

Kaveh, A., Talatahari, S., 2009c. Size optimization of space trusses using big bang-big crunch algorithm. Comput. Struct. 87 (17–18), 1129–1140, [Online]. Available: http://www.sciencedirect.com/science/article/pii/S0045794909001394.

Kaveh, A., Talatahari, S., 2010. Optimal design of skeletal structures via the charged system search algorithm. Struct. Multidiscip. Optim. 41 (6), 893–911, [Online]. Available: http://dx.doi.org/10.1007/s00158-009-0462-5.

Kennedy, J., Eberhart, R.C., 1995. Particle swarm optimization. In: Proceedings of IEEE International Conference on Neural Networks, pp. 1942–1948.

Liang, J.J., Suganthan, P.N., Deb, K., 2005. Novel composition test functions for numerical global optimization. In: Proceedings IEEE Swarm Intelligence Symposium, pp. 68–75.

Lozano, M., Garcia-Martinez, C., 2010. Hybrid metaheuristics with evolutionary algorithms specializing in intensification and diversification: Overview and progress report. Comput. Oper. Res. 37 (3), 481–497.

Mezura-Montes, E., Coello, C.A.C., 2005. Useful Infeasible Solutions in Engineering Optimization with Evolutionary Algorithms. Springer Berlin Heidelberg, pp. 652–662.

Mirjalili, S., 2016. Sca: A sine cosine algorithm for solving optimization problems. Knowl.-Based Syst. 96, 120–133, [Online]. Available: http://www.sciencedirect.com/science/article/pii/S0950705115005043.

Mirjalili, S., Mirjalili, S.M., Hatamlou, A., 2016. Multi-verse optimizer: A nature-inspired algorithm for global optimization. Neural Comput. Appl. 27 (2), 495–513, [Online]. Available: http://dx.doi.org/10.1007/s00521-015-1870-7.

Mirjalili, S., Mirjalili, S.M., Lewis, A., 2014. Grey wolf optimizer. Adv. Eng. Softw. 69, 46–61, [Online]. Available: http://www.sciencedirect.com/science/article/pii/S0965997813001853.

Rashedi, E., Nezamabadi-pour, H., Saryazdi, S., 2009. GSA: A gravitational search algorithm. Inf. Sci. 197 (31), 2232–2248, [Online]. Available: http://www.sciencedirect.com/science/article/pii/S0020025509001200.

Schutte, J., Groenwold, A., 2003. Sizing design of truss structures using particle swarms. Struct. Multidiscip. Optim. 25 (4), 261–269, [Online]. Available: http://dx.doi.org/10.1007/s00158-003-0316-5.

Singh, P., Dhiman, G., 2017. A fuzzy-lp approach in time series forecasting. In: International Conference on Pattern Recognition and Machine Intelligence. Springer, pp. 243–253.

Singh, P., Dhiman, G., 2018a. A hybrid fuzzy time series forecasting model based on granular computing and bio-inspired optimization approaches. J. Comput. Sci. 27, 370–385.

Singh, P., Dhiman, G., 2018b. Uncertainty representation using fuzzy-entropy approach: Special application in remotely sensed high-resolution satellite images (rshrsis). Appl. Soft Comput. 72, 121–139.

Singh, P., Dhiman, G., Guo, S., Maini, R., Kaur, H., Kaur, A., Kaur, H., Singh, J., Singh, N., 2019. A hybrid fuzzy quantum time series and linear programming model: Special application on taiex index dataset. Modern Phys. Lett. A 34 (25).

Singh, P., Dhiman, G., Kaur, A., 2018a. A quantum approach for time series data based on graph and schrödinger equations methods. Modern Phys. Lett. A 33 (35).

Singh, P., Rabadiya, K., Dhiman, G., 2018b. A four-way decision-making system for the indian summer monsoon rainfall. Mod. Phys. Lett. B 32 (25).

Verma, S., Kaur, S., Dhiman, G., Kaur, A., 2018. Design of a novel energy efficient routing framework for wireless nanosensor networks. In: 2018 First International Conference on Secure Cyber Computing and Communication (ICSCCC). IEEE, pp. 532–536.

Wolpert, D.H., Macready, W.G., 1997. No free lunch theorems for optimization. IEEE Trans. Evol. Comput. 1 (1), 67–82.

Yang, X.-S., 2010. Firefly algorithm stochastic test functions and design optimisation. Int. J. Bio-Inspired Comput. 2 (2), 78–84, [Online]. Available: http://dx.doi.org/10.1504/IJBIC.2010.032124.